Survey Paper

Respiratory motion models: A review

J.R. McClelland [a,*], D.J. Hawkes [a], T. Schaeffter [b,c], A.P. King [b,c]

[a] Centre for Medical Image Computing, University College London, Front Engineering Building, Gower Street, London WC1E 6BT, UK
[b] Division of Imaging Sciences and Biomedical Engineering, King's College London, 4th Floor Lambeth Wing, St. Thomas' Hospital, London SE1 7EH, UK
[c] NIHR Biomedical Research Centre at Guy's & St. Thomas' NHS Foundation Trust and King's College London, UK

ARTICLE INFO

ABSTRACT

The problem of respiratory motion has proved a serious obstacle in developing techniques to acquire images or guide interventions in abdominal and thoracic organs. Motion models offer a possible solution to these problems, and as a result the field of respiratory motion modelling has become an active one over the past 15 years. A motion model can be defined as a process that takes some surrogate data as input and produces a motion estimate as output. Many techniques have been proposed in the literature, differing in the data used to form the models, the type of model employed, how this model is computed, the type of surrogate data used as input to the model in order to make motion estimates and what form this output should take. In addition, a wide range of different application areas have been proposed. In this paper we summarise the state of the art in this important field and in the process highlight the key papers that have driven its advance. The intention is that this will serve as a timely review and comparison of the different techniques proposed to date and as a basis to inform future research in this area.

© 2012 Elsevier B.V. All rights reserved.

1. Introduction

Advances in imaging technology in recent decades have opened up an increasingly wide range of potential applications for medical images, including diagnosis, treatment planning and image-guided interventions. However, in the thorax and abdomen the problem of organ motion caused by respiration remains a limiting factor. In image acquisition it can cause artefacts in the acquired images (Nehmeh and Erdi, 2008; Scott et al., 2009), thus limiting their practical utility; whereas in image-guided interventions it can cause a misalignment between the static guidance information and the moving anatomy (Hawkes et al., 2005), limiting the accuracy of the guidance.

A number of solutions have been proposed to deal with the problem of respiratory motion. The simplest approach is breath-holding, but this limits acquisition/intervention time to typically less than 30 s, which is inadequate for many situations. Respiratory gating involves only acquiring/using imaging data during a limited window (e.g. end-expiration), based on a simple respiratory signal. However, this significantly increases acquisition/intervention time. An alternative solution is motion tracking. As it can be difficult to image the motion of interest directly during the procedure, markers are often implanted into the region of interest and tracked using an imaging device such as X-ray (Shirato et al., 2000, e.g.). In this case the implantation can be invasive and motion informa-

tion is only available at the marker(s) and not for the whole region of interest.

Because of the limitations and drawbacks of these techniques, over the past 15 years there has been significant interest in the development of models that can estimate and correct for the effects of respiratory motion. Such models attempt to model the relationship between the motion of interest, i.e. the motion of the internal organ(s), and some 'surrogate' data, e.g. the displacement of the skin surface. This relationship is used to estimate the motion based on the subsequent acquisition of the surrogate data. A wide range of different techniques have been proposed for respiratory motion modelling. This paper reviews progress made and attempts to summarise the current state of the art with a view to informing the direction of future research.

1.1. Scope of the paper

Before reviewing the algorithmic components and techniques involved in forming respiratory motion models, it is first necessary to clearly define what is meant by such a model. The term 'motion model' has been used in the literature to refer to a number of different concepts, including a series of geometric transformations to different respiratory positions, both with (Rit et al., 2009) and without (Li et al., 2006b; Rohlfing et al., 2004; Zhu et al., 2010) interpolation between them.

In this paper we follow the majority of the literature and use the following definition: a motion model refers to a process that takes some surrogate data as input and produces a motion estimate as

---

* Corresponding author. Tel.: +44 2076790177; fax: +44 2076790255.
  E-mail address: j.mcclelland@cs.ucl.ac.uk (J.R. McClelland).

output. Motion models are used when it is not possible or practical to directly measure the actual motion of interest with sufficient temporal resolution during the intended procedure (e.g. image acquisition or an image-guided intervention). If the motion can be directly measured then a motion model is not required as motion tracking can be used. When a motion model is used, measurements are made of some surrogate data instead of measuring the motion of interest directly. The surrogate data should be easily measurable and have a strong relationship with the motion of interest. If this relationship can be modelled then the motion of interest can be estimated from the surrogate data. Examples of different sources of surrogate data used in the literature are given in Section 3.

Typically the motion model is based on motion measurements made from imaging data. When forming the model, the surrogate data is normally acquired at the same time as the imaging data (or can be easily derived from the imaging data). The model then approximates the relationship between the surrogate data and the motion of interest. To apply the model only the surrogate data needs to be acquired, and the model estimates the motion from the current surrogate data. This is illustrated in Figs. 1 and 2. The motion model should be capable of making a motion estimate for any value of the surrogate data (although often within a defined range).

Therefore, according to this definition Li et al. (2006b), Rohlfing et al. (2004), and Zhu et al. (2010) are not classified as motion models, as they only make motion estimates at a number of discrete respiratory positions; whereas Rit et al. (2009) is classified as a motion model, as the proposed technique is capable of interpolating a motion estimate between these discrete positions.

1.1.1. Types of correspondence

The goal of the motion model is to approximate the relationship between the surrogate data and the estimated motion by establishing a correspondence model. This correspondence can be 'direct' or 'indirect'.

1.1.1.1. Direct correspondence. For a direct correspondence the model estimates the motion as a direct function of the surrogate data as illustrated in Fig. 2a (e.g. King et al., 2009a; Manke et al., 2003). Formally, we can write,

$$\mathbf{M} = \phi(\mathbf{s}), \tag{1}$$

where $\mathbf{s}$ is the surrogate data, ϕ the direct correspondence model and $\mathbf{M}$ the estimate of the motion (i.e. a vector of motion parameter estimates). In this case the number of degrees of freedom of the model is determined by the number and nature of the surrogate data, $\mathbf{s}$. The surrogate values directly parameterise the motion estimates and determine what type of motion can be estimated.

1.1.1.2. Indirect correspondence. An indirect correspondence model parameterises the motion using a number of *internal variables* which define the degrees of freedom of the motion model (see Fig. 2b). These variables can have a physiological interpretation, e.g. position in the respiratory cycle (Blackall et al., 2005), or can be a more abstract parameterisation of the motion, e.g. the weights of a statistical model built using principal component analysis (PCA) (King et al., 2012). When the motion model is used to estimate the motion the internal variables are not directly measured. Rather, the surrogate data is a subset of, or can be derived from, the motion estimates made by the model. To apply the motion model the internal variables are optimised to find the best match between the measured surrogate data and the estimates of the surrogate data made by the motion model. Techniques based on indirect correspondence models have sometimes been referred to as 'image-driven' approaches in the literature because, to date, they have always used images as the surrogate data, although this need not necessarily be the case.
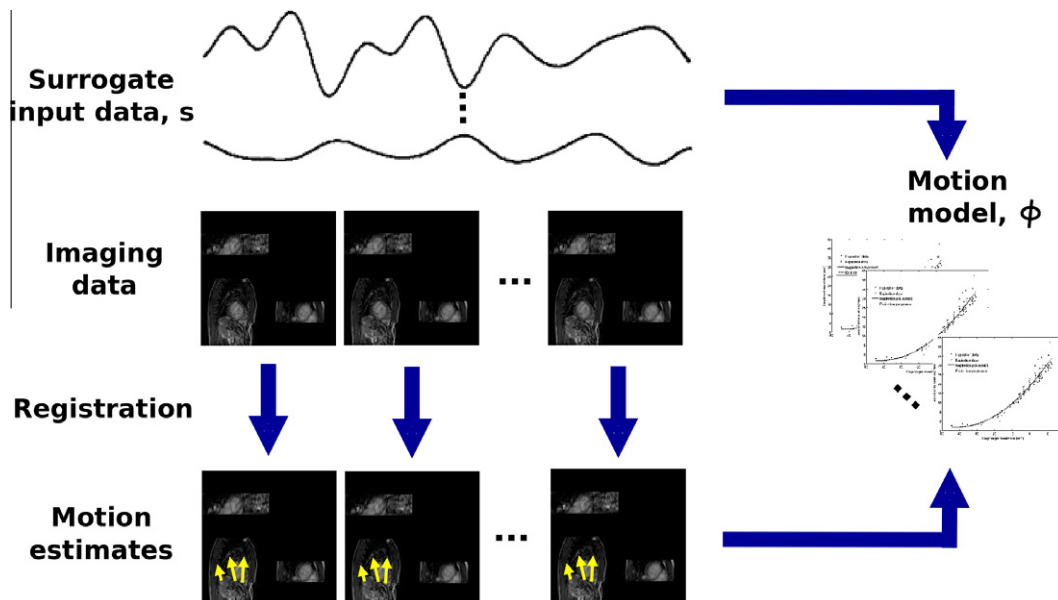
Formally, we can write,

$$\mathbf{M} = \phi(\hat{\mathbf{x}}), \tag{2}$$

where

$$\hat{\mathbf{x}} = \underset{\mathbf{x}}{\operatorname{argmax}} \; Sim(F(T(I, \phi(\mathbf{x}))), \mathbf{s}), \tag{3}$$

in which $\mathbf{x}$ is the vector of internal variables, $\phi(\mathbf{x})$ is a vector of motion parameters estimated from the internal variables, I is a reference image, T is a function that transforms the reference image

Fig. 1. An illustration of the typical formation of a respiratory motion model. Surrogate data is acquired at the same time as some imaging data that represents the organ(s) of interest at different respiratory positions. The motion is estimated from the imaging data, e.g. using image registration, and the motion model approximates the relationship between the surrogate data and the motion.
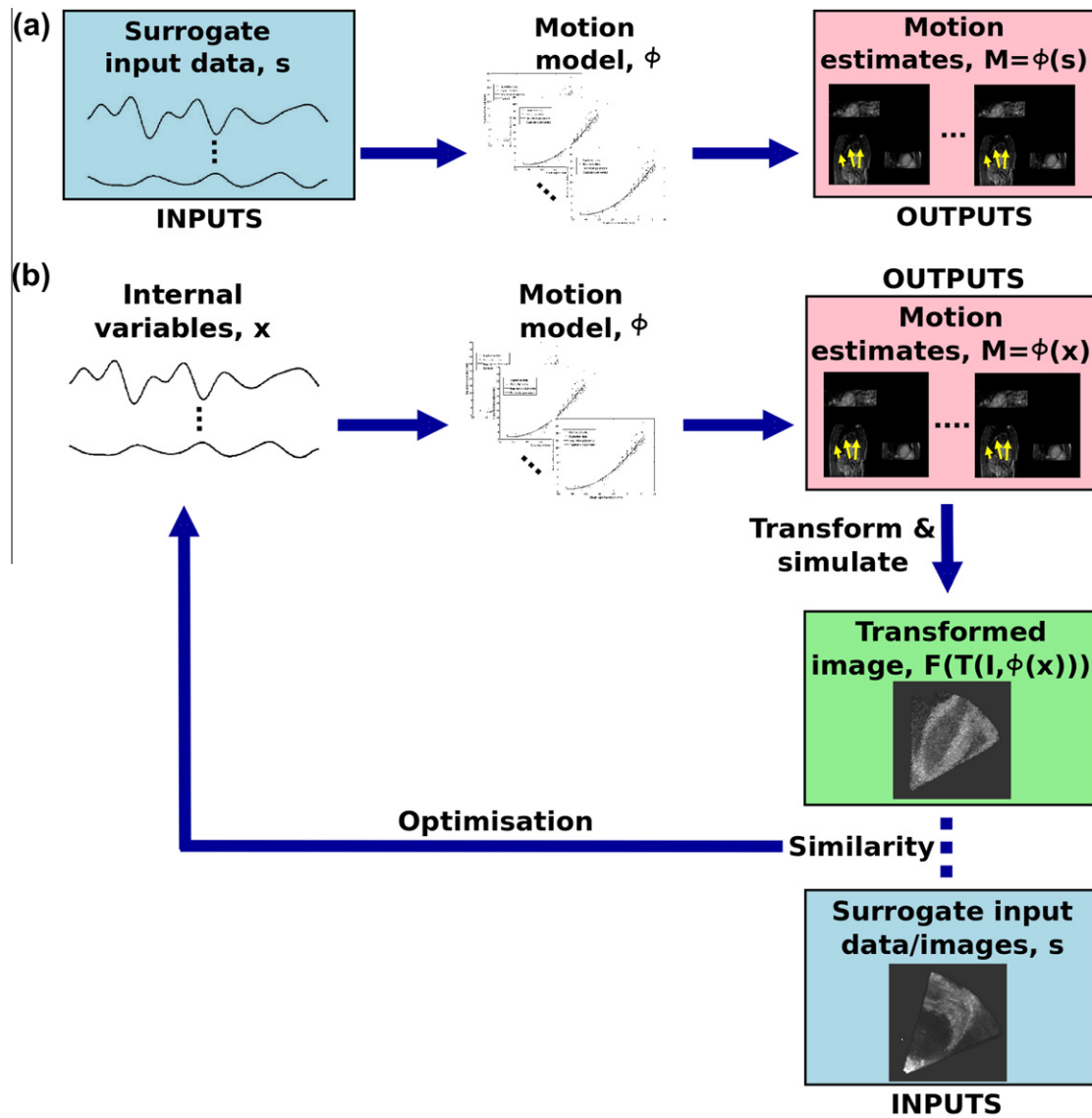
Fig. 2. An illustration of the application of respiratory motion models using direct (a) and indirect (b) correspondence models. A direct correspondence model estimates the motion as a direct function of the surrogate data. An indirect correspondence model parameterises the motion using a number of *internal variables* which are optimised to give the best match between the observed surrogate data and surrogate data simulated from the transformed reference image.

according to the motion parameters, F is a function which simulates the surrogate data from the transformed reference image, and *Sim* is a measure of similarity between the simulated surrogate data and the measured surrogate data, **s**. The function F can vary: it can select a subset of the transformed reference image data corresponding to the surrogate data (King et al., 2008b; King et al., 2010b; Peressutti et al., 2012), or it can simulate the surrogate imaging modality if this is different to the modality used to acquire the reference volume (Blackall et al., 2005; King et al., 2001, 2010c; Li et al., 2011a; Vandemeulebroucke et al., 2009), e.g. simulating an ultrasound (US) signal from a magnetic resonance (MR) volume (Blackall et al., 2005). The internal variables are optimised to find the values, $\hat{\mathbf{x}}$, that produce the best value of *Sim*. →doR2.2 The final motion estimate, **M**, is produced by applying the model ϕ using the values $\hat{\mathbf{x}}$.

1.1.2. Anatomy

This paper will review work carried out to model the respiratory motion of any organ affected by breathing. Predominantly, this means the lungs, the heart and the liver, although work has also been performed to model the respiratory motion of other thoracic organs (see Section 2.1 for a more detailed discussion). In the heart there is the additional problem of motion due to the beating of the heart (which we term cardiac cycle motion). This motion is also approximately repeatable and there are a number of examples of models of cardiac cycle motion in the literature (e.g. Huang et al., 1999). Such models often employ similar modelling techniques to respiratory motion models. Nevertheless, for reasons of clarity and brevity we do not discuss such work in this review. There are also a small number of examples of joint models of both respiratory and cardiac cycle motion (e.g. Odille et al., 2008a, 2010; Shechter et al., 2006). Since these works model breathing motion and are small in number we do include such papers in this review.

1.1.3. Estimation vs. prediction

Due to some inconsistency in the use of terminology in the literature we wish to clarify the use of the terms motion 'estimation' and 'prediction'. The term 'prediction' has been commonly used to refer to estimating the value of a future signal value based on current and/or past values, for example using a technique such as a

Kalman filter (Kalman, 1960). Good reviews of such prediction techniques can be found in Ernst and Schweikard (2009) and Verma et al. (2011). However, the term 'prediction' has also been used to refer to estimating current values (e.g. motion fields) based on some other simple signals (e.g. surrogate values) (Ahn et al., 2004; Cervino et al., 2009, 2010; Ehrhardt et al., 2010). Whilst we do not disagree with such use, for the purpose of this review it is necessary to have some clarity in definitions. Therefore, in this paper we use the term motion 'estimation' to refer to the estimates of current motion made by the type of motion model described above, and 'prediction' to refer to estimating future values of a signal. The subject of this review is models for motion estimation, not motion prediction. However, it should be noted that prediction and estimation can be performed simultaneously. For example, in Isaksson et al. (2005) a motion model was described that could predict future motion estimates based on current surrogate data. This type of approach can be useful, for example, in overcoming latency in motion compensation systems.

1.2. Respiratory motion and its variation

Respiratory motion is often assumed to be, at least approximately, the same from cycle to cycle. To a large extent, this assumption is valid, but there are certain variations in breathing motion that should be discussed and defined with relation to the physiology literature. There are two physiological causes of respiration: contraction of the thoracic diaphragm muscle and movement of the rib cage caused by the rib cage muscles (primarily the internal and external intercostals) (West, 2004). These combined effects cause an increase in intrathoracic volume and a consequent inhalation of air into the lungs (De Troyer and Estenne, 1984; West, 2004). The relative contributions of these two causes can vary from breathing cycle to breathing cycle, and can differ greatly depending on the subject's pose (e.g. supine/upright) (De Troyer and Estenne, 1984; Sharp et al., 1975) and breathing pattern (e.g. deep/shallow) (Sharp et al., 1975). Significant variation also exists between individuals (Konno and Mead, 1967). The existence of these two underlying causes of respiration and their variability means that the motion of organs due to respiration is not perfectly repeatable (Benchetrit, 2000): changes in the relative contributions and their magnitudes cause breathing motion to be slightly different during each breathing cycle. This fact has been confirmed by a number of empirical studies of breathing variation based on imaging data (Blackall et al., 2006; Hughes et al., 2008; McClelland et al., 2011).

Based on this, we now define a number of key terms regarding breathing variation:

- *Intra-cycle variation:* This refers to variation of motion within a single breathing cycle, i.e. the motion path followed during inspiration is different to that followed during expiration. This is often referred to as *hysteresis* in the literature;
- *Inter-cycle variation:* This refers to variation of motion *between* breathing cycles, i.e. the motion path followed during one breathing cycle is different to that followed during another breathing cycle.

In addition, in applications such as radiotherapy (RT), the variation in motion within and between treatment *fractions* is of interest (Sonke et al., 2008):

- *Intra-fraction variation:* This refers to variation of motion within a single fraction, or treatment session;
- *Inter-fraction variation:* This refers to variation of motion between fractions, potentially over a period of days or weeks.

These two concepts are related to that of inter-cycle variation since they refer to variation in motion between cycles. However, the two types of variation need to be addressed in different ways. Intra-fraction variation can potentially be included in the model and estimated from the surrogate data. Estimating inter-fraction variation from surrogate data is prone to error as it is often difficult and sometimes impossible to know how the surrogate data from one fraction corresponds to the surrogate data from another fraction (McClelland et al., 2011).

1.3. Structure of this paper

The remainder of this paper is structured as follows. In Section 2 we review the range of applications and organs for which respiratory motion models have been proposed. In Section 3 techniques for acquiring surrogate data to act as inputs to motion models are detailed. Section 4 describes methods for acquiring motion information and reviews imaging modalities that have been used as sources of such information. In Section 5 we categorise and describe the different modelling approaches that have been employed. Finally, Section 6 discusses the current state of the art and offers some speculation about fruitful future directions.

2. Uses of motion models

Respiratory motion models, as defined in the previous section, have been proposed for use in a wide range of clinical applications and for several different anatomical regions in the thorax/abdomen. In this section we review these applications and anatomical regions.

2.1. Anatomy

Table 1 summarises the anatomical/pathological regions for which the use of respiratory motion models has been proposed. As can be seen, the most common regions proposed to date have been the lungs, the heart, and the liver. The predominance of these regions has been driven mainly by three of the most popular applications for which respiratory motion is a problem: radiotherapy, minimally invasive cardiac interventions and liver ablation (see Section 2.2).

Note that there have been a number of motion models proposed in the literature for modelling general respiratory motion anywhere in the thorax/abdomen rather than just modelling the motion for one specific organ, as can be seen in the first row of Table 1. However, only some of these were validated on data from multiple organs (Cho et al., 2008, 2010, 2011; Isaksson et al., 2005; King et al., 2011, 2012; Schweikard et al., 2004a; Torshabi et al., 2010; Zhang et al., 2010). Others were validated using data from just a single organ (Geneser et al., 2011; Ruan et al., 2008; Schweikard et al., 2000; Seppenwoolde et al., 2007) or using data simulated from a computer phantom (Rahni et al., 2011).

2.2. Applications

Table 2 summarises the different applications that motion models have been proposed for. The proposed clinical applications of respiratory motion models can be divided into two broad categories: image-guided interventions and image acquisition. In image-guided interventions respiratory motion can cause a misalignment between the static guidance information and the moving anatomy. This can lead to misleading guidance information or errors in treatment delivery/planning. Motion models can reduce the severity of such problems. In image acquisition, respiratory motion can cause artefacts in the acquired images. The

Table 1
A summary of the anatomical/pathological regions for which the use of respiratory motion models has been proposed.

Organ	Examples
Thorax/abdomen (not organ-specific)	*Just tumour:* Schweikard et al., 2000; Schweikard et al., 2004a; Schweikard et al., 2004b; Isaksson et al., 2005; Schweikard et al., 2005; Seppenwoolde et al., 2007; Cho et al., 2008; Ruan et al., 2008; Cho et al., 2010; Torshabi et al., 2010; Cho et al., 2011 *General organ(s):* Fayad et al., 2010; Zhang et al., 2010; Geneser et al., 2011; King et al., 2011; Rahni et al., 2011; King et al., 2012
Lungs	*Just tumour:* Ahn et al., 2004; Hoisak et al., 2004; Berbeco et al., 2005; Chi et al., 2006; Meyer et al., 2006; Ionascu et al., 2007; Cervino et al., 2009; Hoogeman et al., 2009; Cervino et al., 2010; Martin et al., 2012 *General lungs:* Koch et al., 2004; Liu et al., 2004; Sundaram et al., 2004; Low et al., 2005; McClelland et al., 2005; Plathow et al., 2005; Blackall et al., 2006; Li et al., 2006b; Li et al., 2006a; McClelland et al., 2006; Ehrhardt et al., 2007; McClelland et al., 2007; Reyes et al., 2007; Zhang et al., 2007; Colgan et al., 2008; Ehrhardt et al., 2008; Gao et al., 2008; Odille et al., 2008a; Yang et al., 2008; Fayad et al., 2009b; Fayad et al., 2009c; Fayad et al., 2009a; Klinder et al., 2009; Rit et al., 2009; Vandemeulebroucke et al., 2009; Zhao et al., 2009; Ehrhardt et al., 2010; He et al., 2010; Klinder et al., 2010; Liu et al., 2010; Low et al., 2010; Ehrhardt et al., 2011; Fayad et al., 2011; Li et al., 2011a; Li et al., 2011b; McClelland et al., 2012
Heart	*General heart:* Atkinson et al., 2001; McLeish et al., 2002; Buliev et al., 2003; Ablitt et al., 2004; Timinger et al., 2004; Wu et al., 2006; Jahnke et al., 2007; Sharif and Bresler, 2007; Odille et al., 2008b; Odille et al., 2008a; King et al., 2008b; King et al., 2009a; King et al., 2009b; King et al., 2010b; King et al., 2010c; King et al., 2010a; Odille et al., 2010; Filipovic et al., 2011; McGlashan and King, 2011; Savill et al., 2011; Peressutti et al., 2012 *Left ventricle:* Nehrke et al., 2001 *Coronary arteries:* Wang et al., 1995; Manke et al., 2002a; Manke et al., 2002b; Manke et al., 2003; Shechter et al., 2004; Jahnke et al., 2005; Nehrke and Bornert, 2005; Shechter et al., 2005; Fischer et al., 2006; Shechter et al., 2006; Schneider et al., 2010
Liver	*General liver:* Blackall et al., 2001; King et al., 2001; Blackall et al., 2005; Odille et al., 2008b; Odille et al., 2008a; Hinkle et al., 2009; White et al., 2009; Rijkhorst et al., 2010; Rijkhorst et al., 2011; Buerger et al., 2012; Preiswerk et al., 2012 *Portal vein:* Khamene et al., 2004 *Implanted fiducials:* Beddar et al., 2007; Ernst et al., 2009 *Vessel bifurcations:* Ernst et al., 2011
Kidney	Odille et al., 2008b
Diaphragm	Vedam et al., 2003; McQuaid et al., 2009; McQuaid and Lambrou, 2011

Table 2
A summary of the different clinical applications that motion models have been proposed for.

Category	Application	Examples
Image guided interventions	Radiotherapy	Schweikard et al., 2000; Vedam et al., 2003; Ahn et al., 2004; Hoisak et al., 2004; Koch et al., 2004; Liu et al., 2004; Schweikard et al., 2004a; Schweikard et al., 2004b; Berbeco et al., 2005; Isaksson et al., 2005; Low et al., 2005; McClelland et al., 2005; Plathow et al., 2005; Schweikard et al., 2005; Blackall et al., 2006; Chi et al., 2006; McClelland et al., 2006; Meyer et al., 2006; Beddar et al., 2007; Ionascu et al., 2007; McClelland et al., 2007; Zhang et al., 2007; Cho et al., 2008; Colgan et al., 2008; Gao et al., 2008; Ruan et al., 2008; Yang et al., 2008; Cervino et al., 2009; Ernst et al., 2009; Fayad et al., 2009c; Fayad et al., 2009b; Hoogeman et al., 2009; Vandemeulebroucke et al., 2009; Cervino et al., 2010; Cho et al., 2010; Liu et al., 2010; Torshabi et al., 2010; Cho et al., 2011; Ernst et al., 2011; Li et al., 2011a; Li et al., 2011b; McClelland et al., 2011; Martin et al., 2012
	Cardiac catheterisation	Shechter et al., 2004; Timinger et al., 2004; Shechter et al., 2005; Shechter et al., 2006; King et al., 2009a; King et al., 2009b; King et al., 2010b; King et al., 2010c; Schneider et al., 2010; McGlashan and King, 2011; Savill et al., 2011; Peressutti et al., 2012
	Liver ablations	*Radiofrequency:* Blackall et al., 2001; King et al., 2001; Blackall et al., 2005; Preiswerk et al., 2012 *HIFU:* Rijkhorst et al., 2010; Rijkhorst et al., 2011
	Bronchoscopy	Klinder and Lorenz, 2012
Image acquisition	MR	Wang et al., 1995; Nehrke et al., 2001; Manke et al., 2002b; Manke et al., 2002a; Manke et al., 2003; Jahnke et al., 2005; Nehrke and Bornert, 2005; Fischer et al., 2006; Jahnke et al., 2007; Sharif and Bresler, 2007; Odille et al., 2008b; Odille et al., 2008a; White et al., 2009; Odille et al., 2010; Filipovic et al., 2011
	PET	Reyes et al., 2007; McQuaid et al., 2009; Fayad et al., 2010; Ambwani et al., 2011; King et al., 2011; McQuaid and Lambrou, 2011; Rahni et al., 2011; King et al., 2012
	CT	*4-D CT:* McClelland et al., 2006; Ehrhardt et al., 2007; Hinkle et al., 2009; McClelland et al., 2011 *CBCT:* Buliev et al., 2003; Rit et al., 2009; Zhang et al., 2010; Martin et al., 2012
	Fluoroscopy	Shechter et al., 2005
	US	Atkinson et al., 2001
Other	Quantification and analysis	Blackall et al., 2001; McLeish et al., 2002; Shechter et al., 2004; Shechter et al., 2006; Zhao et al., 2009; Low et al., 2010
	Computational phantom	Segars et al., 2001

nature of the artefacts depends on the nature of the imaging modality, but any imaging modality in which there is significant motion during acquisition of an image will suffer from such artefacts.

2.2.1. Image-guided interventions

One of the main image-guided interventions for which motion models have been proposed is radiotherapy. Radiotherapy involves directing beams of ionising radiation towards tumours with the aim of killing the cancerous cells and leaving surrounding healthy tissue intact. However, for tumours in thoracic/abdominal areas

such as the lungs and liver, respiratory motion can cause the tumour to move during radiotherapy treatment. For this reason extra margins are added to the radiotherapy target to account for the expected respiratory motion (Keall et al., 2006). However, the use of margins causes the surrounding healthy tissue to receive more dose than it would if the target was static, and if the margins used are inadequate the tumour may receive less dose than intended. Therefore active treatments have been proposed such as gated or tracked treatments (Keall et al., 2006). In gated treatments the radiotherapy beam is only turned on for a fraction of the respiratory cycle, minimising the effects of respiratory motion but

increasing the treatment time. In tracked treatments the radiotherapy beam is made to follow the motion of the tumour, minimising both the treatment time and the effects of respiratory motion.

Motion models have been proposed for a number of uses in radiotherapy, including: accounting for respiratory motion when planning margin based treatments (Blackall et al., 2006; Colgan et al., 2008; Geneser et al., 2011), setting up patients and checking the plan is still valid (Li et al., 2011a; Vandemeulebroucke et al., 2009), and for planning and guiding gated or tracked treatments (e.g. Berbeco et al., 2005; Schweikard et al., 2000). Schweikard et al. (2000) was the first paper to propose using respiratory motion models to guide RT treatment, although they only modelled the motion of a single point of interest (a marker implanted in the tumour), and used a very simple model. Low et al. (2005) was the first to propose a motion model for RT treatment that could potentially model intra- and inter-cycle variation. Blackall et al. (2006) and McClelland et al. (2006) were the first to propose motion models for RT that could model an entire region of interest, using affine and deformable transformations respectively.

In image-guided cardiac interventions such as cardiac catheterisations (Grossman, 1986) the only imaging data routinely available for intraprocedure motion estimation is fluoroscopic X-ray. Fluoroscopy images are 2-D, which would limit the dimensionality of any motion estimate directly derived from such images. Biplane systems do exist but they are not currently widespread in clinical use. Furthermore, fluoroscopy images are normally only useful for visualising catheters, guidewires and other instruments due to their low signal-to-noise ratio and poor contrast within soft tissue structures such as the heart chambers and major vessels. Injection of an iodine-based contrast medium can briefly highlight such structures but the contrast medium is mildly toxic to the kidneys and washes out within a few seconds of injection. Therefore, the use of fluoroscopy images for 3-D motion estimation remains extremely challenging and motion models offer an attractive alternative solution. Models have been proposed that are formed from MR imaging (King et al., 2009a,b, 2010b; Peressutti et al., 2012), contrast-enhanced X-ray images (Schneider et al., 2010; Shechter et al., 2004, 2005, 2006) or even magnetic tracking data (Timinger et al., 2004). A significant early work was that of Shechter et al. (2005), who used a motion model derived from contrast-enhanced X-ray to correct subsequent non-enhanced X-ray images for the effects of respiratory and cardiac cycle motion. An alternative approach is to use the model to update a roadmap derived from a static preprocedure scan to account for respiratory motion. This was first demonstrated in King et al. (2009a) using a MR derived motion model. Subsequent related work includes King et al. (2009b, 2010b,c), McGlashan and King (2011), Peressutti et al. (2012), Savill et al. (2011), and Schneider et al. (2010).

A further application of respiratory motion models in image-guided interventions is in ablation of metastases, usually arising in the liver, using radiofrequency (McGahan et al., 1990) or high intensity focused ultrasound (HIFU) (Lynn et al., 1942). Radiofrequency ablation involves inserting a needle-like ablation probe into the target region (e.g. the tumour) and thermally ablating it to destroy cancerous tissue. HIFU is a less invasive alternative in which a focused US beam is used to heat the tumour. Radiofrequency ablation is normally guided using US images, which have poor signal-to-noise ratio making motion estimation challenging. HIFU, on the other hand, can be guided using MR (Cline et al., 1992) as well as US data. However, the speed of MR imaging is not currently sufficient to deliver 3-D motion information with sufficient temporal resolution for guidance purposes. Therefore motion models have been proposed to provide motion estimates with higher temporal resolution. A key work here was that of Blackall et al. (2005), who built on the earlier preliminary work in Blackall et al. (2001) and King et al. (2001) to propose a system

based on a MR derived motion model and intraprocedure US images. More recent work has been carried out by Rijkhorst et al. (2010) and Rijkhorst et al. (2011).

2.2.2. Image acquisition

In image acquisition one of the main modalities for which motion models have been proposed is MR. In MR, motion can lead to blurring or ghosting artefacts in the acquired images (Wood and Henkelman, 1985). In particular, respiratory motion compensation is a well-known requirement for cardiac and abdominal MR and various methods for monitoring respiration have been suggested including a bellows or MR navigator echoes (see Section 3). Apart from respiratory gating, these measurements can be used to reduce and/or to correct for respiratory motion in either a prospective or retrospective way.

In prospective correction a motion estimate is used to scale the magnetic field gradients during image acquisition to compensate for the effects of the motion on the acquired k-space data. Such corrections are limited to linear transformations (i.e. at most affine) due to the linear nature of the magnetic field gradient system. In retrospective correction the acquired k-space data is postprocessed to remove the effects of motion. Such corrections are not limited to linear transformations (Batchelor et al., 2005) but the correction can be computationally demanding (Manke et al., 2002a; Odille et al., 2008b).

In both the prospective and retrospective cases an accurate motion estimate is required to make the necessary corrections. Motion models have been proposed for providing such estimates in both approaches. A key early work was that of Wang et al. (1995), who proposed using a linear relationship between the diaphragm translation and the translation of a small imaging slab covering the coronary arteries. This can be viewed as a simple generic motion model. Subsequently models that could estimate more realistic motions (i.e. affine, nonlinear) were proposed. The first paper to propose a technique for prospective affine motion correction in MR was Manke et al. (2002b), and demonstration of such a technique in a clinical MR scanner was shown in Nehrke and Bornert (2005). Other related works include Fischer et al. (2006), Jahnke et al. (2005), and Manke et al. (2003). For retrospective correction, the mathematical theory for nonlinear motion was described in Batchelor et al. (2005) and first applied using a motion model based technique in Odille et al. (2008b). Subsequent works include Filipovic et al. (2011), Odille et al. (2008a), Odille et al. (2010), and White et al. (2009). In addition, a number of general motion models have been proposed without being specific about which motion-correction strategy they could be used for (Jahnke et al., 2007; Manke et al., 2002a; Nehrke et al., 2001; Sharif and Bresler, 2007; Wang et al., 1995).

Positron emission tomography (PET) images are acquired as projections which are then reconstructed using either analytic or iterative techniques. Motion causes blurring artefacts in the reconstructed images (Nehmeh and Erdi, 2008). Motion correction can be performed in one of three ways. First, in *line-of-response* (LOR) correction the motion corrections are made to the *list-mode* data (i.e. the list of coincidence events) (Chung et al., 2008). Such corrections are limited to transformations that preserve straight lines so, at most, affine transformations can be used. Second, in *motion-corrected image reconstruction* (MCIR) the motion estimate is incorporated into the system matrix of the reconstruction. MCIR techniques can incorporate nonrigid motion corrections. Finally, in *reconstruct-transform-average* (RTA) a number of gated PET images are reconstructed separately and motion estimates used to motion correct each gate, followed by an averaging of all motion corrected images. RTA techniques can also incorporate nonrigid transformations. Motion models have been proposed to provide the motion estimates for MCIR (Ambwani et al., 2011; Fayad

et al., 2010; Reyes et al., 2007) and RTA (King et al., 2011; King et al., 2012), but to the authors' knowledge, no motion model based technique has been proposed using LOR correction. In addition, a number of motion model techniques have been proposed for use in PET imaging without being specific as to which motion correction approach they are intended for (McQuaid et al., 2009; McQuaid and Lambrou, 2011; Rahni et al., 2011).

4-D computed tomography (4-D CT) scans have become very popular for imaging respiratory motion. They generate a number of CT volumes representing different points in the respiratory cycle. During a single breathing cycle there is only enough time to acquire data from a limited field of view. Therefore, data is acquired over several cycles and then sorted or 'binned' using a surrogate signal (see Section 3) to form full volumes representing a single respiratory cycle (Keall et al., 2004; Pan et al., 2004). 4-D CT volumes will often contain artefacts due to the need to bin the data, and inter-cycle variation during the acquisition. Motion models have been proposed to address both these issues and reduce the artefacts in the 4-D CT volumes (Ehrhardt et al., 2007; Hinkle et al., 2009; McClelland et al., 2006, 2011).

On-board Cone Beam CT (CBCT) imaging is now widely used for setting up radiotherapy patients. An X-ray source and detector are mounted on the same gantry as the Linear Accelerator (LINAC) used to deliver the radiotherapy treatment, and can produce a 3-D CT volume of the patient in the treatment position to check that they are set-up correctly. The detector is large enough that it can usually acquire a sufficient volume in a single rotation, but as it is attached to the same gantry as the LINAC it can take approximately 1 min or more to acquire a full volume. Therefore, respiratory motion can cause blurring and other artefacts in the reconstructed volumes. Motion models have been proposed for compensating for respiratory motion when reconstructing CBCT volumes (Buliev et al., 2003; Martin et al., 2012; Rit et al., 2009; Zhang et al., 2010).

Finally a small number of papers have proposed using motion models for motion correcting other imaging modalities. Notable among these are Shechter et al. (2005), who described the use of a motion model derived from biplane contrast-enhanced fluoroscopic X-ray images to motion correct subsequent non-contrast-enhanced fluoroscopy images of the coronary arteries; and Atkinson et al. (2001), who proposed a simple motion model based on the tracking of a passive marker on the subject's abdomen to correct superior–inferior translational motion in US images.

2.2.3. Other applications

Apart from use in image-guided interventions and image acquisition, motion models have been used in several other miscellaneous applications. For example, in Shechter et al. (2004) and Shechter et al. (2006) a motion model was used for quantitative measurement and analysis of the motion of the coronary arteries due to respiration and the beating of the heart. Information about this type of motion can be useful for future development of motion correction techniques, and potentially also for diagnostic purposes. Motion models have also been used for motion pattern analysis in the liver (Blackall et al., 2001), heart (McLeish et al., 2002) and lungs (Low et al., 2010; Zhao et al., 2009).

Another application of motion models has been to create dynamic numerical phantom data for assessment of motion estimation algorithms. In Segars et al. (2001) a time continuous 4-D respiratory motion model was used to transform the MCAT phantom to create a 4-D phantom including different respiratory positions.

Cross-population motion models are formed from motion data acquired from many different subjects, and attempt to capture the nature of breathing motion across the population (Ehrhardt et al., 2011, 2010, 2008; Fayad et al., 2009a; He et al., 2010; Klinder

et al., 2009, 2010, 2012; Preiswerk et al., 2012; Sundaram et al., 2004). This type of model can represent an average motion (Ehrhardt et al., 2008, 2011; Sundaram et al., 2004) or can represent an average motion together with some information about individual variation from the average (Ehrhardt et al., 2010; Fayad et al., 2009a; He et al., 2010; Klinder et al., 2009, 2010, 2012; Preiswerk et al., 2012). Cross-population motion models have a wide range of potential application, including quantitative analysis of motion for diagnostic purposes. In addition, the cross-population model can be adapted to individuals and used for image-guided interventions or image acquisition, resulting in a subject-specific motion model but with reduced need for extra imaging data. However, to date, most cross-population models remain research tools and firm clinical applications have yet to be demonstrated. The different methodological techniques involved in forming cross-population models will be discussed in Section 5.5.

3. Acquiring input surrogate data

In this section the different ways of making physical measurements to be used as surrogate data for respiratory motion models are reviewed. The main requirements for such measurements are that they have a strong relationship with the true motion that the model is intended to estimate, and that they can be acquired relatively easily and with sufficiently high temporal resolution. The surrogate data can be simple scalar values (i.e. a 1-D signal over time (Hoisak et al., 2004; Manke et al., 2002a; Odille et al., 2008b)) or more complex data such as 2-D (Blackall et al., 2005; Vandemeulebroucke et al., 2009) or 3-D (King et al., 2010b) images. Tables 3 and 4 summarise the various possibilities for acquiring such simple or higher dimensional data. The following sections discuss these in more detail.

3.1. Scalar surrogate data

For the application of respiratory motion models in MR image acquisition the most common surrogate data proposed has been the MR navigator echo. This involves a small column of magnetisation being excited to measure the position of a region of tissue over time (Danias et al., 1989). They have been most commonly used to track the head-foot translation of the right hemi-diaphragm, although navigators have also been applied on the anterior chest wall and the lateral wall of the heart for motion modelling purposes. A comparative study to investigate the optimal navigator position(s) for motion modelling has been reported in Manke et al. (2003) (using three different positions).

The respiratory bellows is an alternative means of measuring respiratory position during MR scanning (Santelli et al., 2011). This consists of an air filled bag, which is wedged between the subject's abdomen or chest and a firm surface such as an elasticated belt. The motion of the abdomen or chest during respiration causes air to be expelled from the bellows and a sensor measures the flow of the air. The bellows was originally designed for respiratory gating of MR image acquisition but it is not widely used for this purpose today due to technical issues regarding lack of information about breathing amplitude. It has been applied to generate surrogate data for respiratory motion models, with initial demonstration being shown in Odille et al. (2008b) and subsequent work including (Filipovic et al., 2011; Odille et al., 2008a; Rijkhorst et al., 2010).

A spirometer measures the air flow to and from the lungs, and is commonly used for testing pulmonary function. It has also been proposed for use as a source of surrogate data for respiratory motion models, mainly for the application of motion correction in radiotherapy. This was initially shown by Hoisak et al. (2004)

Table 3
A summary of the means of acquiring input signals for forming and applying motion models: use of scalar or higher dimensional signals.

Surrogate type	Details	Examples
Scalar	MR navigator	*Diaphragm:* Nehrke et al., 2001; Manke et al., 2002b; Manke et al., 2002a; Manke et al., 2003; Jahnke et al., 2005; Nehrke and Bornert, 2005; Fischer et al., 2006; Jahnke et al., 2007; King et al., 2008a; King et al., 2008b; King et al., 2009a; King et al., 2009b; King et al., 2010b; King et al., 2010c; King et al., 2010a; King et al., 2011
		Anterior chest wall: Manke et al., 2003; Jahnke et al., 2005; Nehrke and Bornert, 2005; Jahnke et al., 2007
		Lateral heart wall: Manke et al., 2003; Nehrke and Bornert, 2005; Jahnke et al., 2007
	Bellows	Odille et al., 2008b; Odille et al., 2008a; Rijkhorst et al., 2010; Filipovic et al., 2011
	Spirometer	Hoisak et al., 2004; Low et al., 2005; Lu et al., 2005; Ehrhardt et al., 2007; Yang et al., 2008; Zhao et al., 2009; Low et al., 2010
	Chest/abdomen displacement	*Optical:* Schweikard et al., 2000; Atkinson et al., 2001; Vedam et al., 2003; Schweikard et al., 2004a; Schweikard et al., 2004b; Lu et al., 2005; McClelland et al., 2005; Schweikard et al., 2005; Chi et al., 2006; Li et al., 2006b; Li et al., 2006a; McClelland et al., 2006; Meyer et al., 2006; Beddar et al., 2007; McClelland et al., 2007; Cho et al., 2008; Colgan et al., 2008; Ernst et al., 2009; Fayad et al., 2009c; Hinkle et al., 2009; Hoogeman et al., 2009; Cho et al., 2010; Torshabi et al., 2010; Cho et al., 2011; Ernst et al., 2011; Geneser et al., 2011
		Electromagnetic: Hoisak et al., 2004; Timinger et al., 2004
		Laser: Berbeco et al., 2005; Ionascu et al., 2007; Seppenwoolde et al., 2007; Ruan et al., 2008
Higher dimensional	Surfaces	Ablitt et al., 2004; Wu et al., 2006; Gao et al., 2008; Fayad et al., 2009b; Fayad et al., 2009a; Klinder et al., 2009; Fayad et al., 2010; Klinder et al., 2010; Liu et al., 2010; Rahni et al., 2011
	Images	*CBCT:* Vandemeulebroucke et al., 2009; Li et al., 2011a
		US: King et al., 2001; Blackall et al., 2005; King et al., 2008b; King et al., 2010b; Peressutti et al., 2012
		MR: King et al., 2012
		MR k-space: White et al., 2009

Table 4
A summary of the means of acquiring input signals for forming and applying motion models: use of simpler signals derived from higher dimensional data.

Surrogate type	Details	Examples
Simpler signals derived from higher dimensional data	From fluoroscopy	*Diaphragm:* Shechter et al., 2004; Shechter et al., 2005; Shechter et al., 2006; King et al., 2008a; Cervino et al., 2009; King et al., 2009a; King et al., 2009b; Cervino et al., 2010; Klinder and Lorenz, 2012
		Skin markers: Ahn et al., 2004; Isaksson et al., 2005
		Internal markers: Preiswerk et al., 2012
	From MR	*Diaphragm:* Blackall et al., 2006; McGlashan and King, 2011; Rijkhorst et al., 2011; Savill et al., 2011
		Chest/abdomen: Khamene et al., 2004; Koch et al., 2004; Liu et al., 2004; Plathow et al., 2005; McGlashan and King, 2011; Savill et al., 2011
		Heart wall: McGlashan and King, 2011; Savill et al., 2011
	From MR k-space	Odille et al., 2010; Buerger et al., 2012
	From US	*Diaphragm:* Xu and Hamilton, 2006; Rijkhorst et al., 2010
	From CBCT	*Diaphragm:* Buliev et al., 2003; Rit et al., 2009
	From 4-D CT	*Diaphragm:* Zhang et al., 2007; Zhang et al., 2010
		Chest/abdomen: McClelland et al., 2005; Chi et al., 2006; McClelland et al., 2006; Colgan et al., 2008; He et al., 2010; Fayad et al., 2011
	From skin surface	Hughes et al., 2008; Li et al., 2009; Hughes et al., 2009; McClelland et al., 2011

and also subsequently in (Low et al., 2005, 2010; Yang et al., 2008; Zhao et al., 2009). One problem with using spirometry as a surrogate signal is that there can be considerable drift in the spirometry signal due to instrumentation errors and/or escaping air. To help overcome this problem it has been proposed that another 'drift-free' surrogate signal such as an optical tracking signal (Lu et al., 2005) should be acquired at the same time as the spirometry signal. This can then be used to linearly correct for the drift in the spirometer signal.

A common means of acquiring respiratory surrogate data for a range of motion modelling applications has been to track the motion of one or more points on the surface of the chest or abdomen. This can be done using optical tracking technology such as the Varian Real-time Position Management (RPM)[1] system (Beddar et al., 2007; Chi et al., 2006; Fayad et al., 2009c; Geneser et al., 2011; Hinkle et al., 2009; Li et al., 2006b,a; Vedam et al., 2003). Alternatively electromagnetic tracking systems or laser based tracking systems can also be employed.

There have been a few papers that have compared spirometry and the displacement of a point on the skin surface as potential surrogate signals. They have found that spirometry generally has a better linear correlation with the internal motion than surface displacement (Hoisak et al., 2004; Lu et al., 2005).

3.2. Higher dimensional surrogate data

A number of motion modelling techniques have been proposed that make use of more complex, higher dimensional, data than simple scalar values. These can be broadly categorised into two types of data: surfaces and images.

The full 3-D skin surface can be relatively easily acquired with modern photogrammetry systems such as AlignRT[2] or time of flight cameras. Several papers have proposed using the full skin surface (or at least many surface points) as surrogate data (Ablitt et al., 2004; Fayad et al., 2009b,a, 2010; Gao et al., 2008; Rahni et al., 2011; Wu et al., 2006). However, due to difficulties in acquiring the skin surface data at the same time as the data used to image the internal motion, these papers have extracted the skin surface from the image data rather than measuring it with another system. Some papers have actually acquired skin surface data independently of the internal imaging data (McClelland et al., 2011), but these works extracted a

simple scalar surrogate signal from the surface data rather than using the full surfaces as surrogate data (see Section 3.2.1).

Some authors have proposed using parts of the diaphragm surface (Klinder et al., 2009, 2010, 2012) or the full lung surface (Liu et al., 2010) as surrogate data. While the diaphragm surface could be measured using fluoroscopy or US, it is not clear how the full lung surfaces could be measured during an image guided intervention (Klinder and Lorenz, 2012).

Proposals for using images as surrogate data have included cone beam CT projections (Li et al., 2011a; Vandemeulebroucke et al., 2009); 2-D (Blackall et al., 2005; King et al., 2001) and 3-D (King et al., 2008b, 2010b; Peressutti et al., 2012) US; or a small number of lines of k-space (White et al., 2009) acquired during MR imaging. Although 2D MR 'navigators' are gaining attention in the literature on respiratory motion correction (Henningsson et al., 2012; Keegan et al., 2007; Stehning et al., 2005; Uribe et al., 2007) to the authors' knowledge the only paper to have used such images as surrogate data for a motion model is King et al. (2012). The first description of a motion modelling technique using images as surrogate data was that of King et al. (2001) using 2-D US. Note that in all cases a motion model was required because it was not feasible to estimate the motion directly from the images, either because of a limited amount of data (Blackall et al., 2005; Li et al., 2011a; Vandemeulebroucke et al., 2009; White et al., 2009) or because of poor quality images (King et al., 2010b). All of the above methods were *image driven* approaches, based on *indirect correspondences* (see Sections 1.1.1 and 5.3.2). The high dimensional data was used as input to the motion model, but a much smaller number of internal variables determined the number of degrees of freedom of the model. Alternatively, the images can be preprocessed to extract one or more simple scalar surrogate signals (see Section 3.2.1).

3.2.1. Deriving simpler surrogate data from high dimensional data

As well as being used as higher dimensional surrogate data, both images and surfaces have been used as sources from which to derive simpler surrogate signals. For example, fluoroscopic X-ray images have been used to track skin markers (Ahn et al., 2004; Isaksson et al., 2005) or internal markers (Preiswerk et al., 2012) resulting in a small number of translational motion parameters which can be used as surrogates. Alternatively, the translational motion of a region of the diaphragm has been tracked from fluoroscopic X-ray images, US images, cone beam CT images or 4-D CT images. Chest/abdominal displacement has also been derived from CT images and MR images. The displacement of the lateral and posterior walls of the heart have been derived from MR images in (McGlashan and King, 2011; Savill et al., 2011), which also performed comparative studies to find the optimal MR navigator position(s) for motion modelling.

Also in MR scanning, respiratory signals for motion modelling have been extracted from the central k-space lines, i.e. from the acquired data itself (Buerger et al., 2012; Odille et al., 2010). When orienting the readout direction along the foot-head (FH) direction, the 1-D Fourier transform of the central k-space lines forms a 1-D intensity projection of the 3-D image onto the FH axis. This projection can then be treated in a similar way to a MR navigator and can be used for estimating a scalar respiratory surrogate value for each volume.

Simple scalar surrogate signals have been derived from skin surface data by tracking a single point on the skin surface (Hughes et al., 2009), or by calculating the volumes under the skin surface (Hughes et al., 2009; Li et al., 2009; McClelland et al., 2011). It has been shown that calculating the volume under the skin surface produces a signal similar to that obtained via spirometry, but without the drift often seen in spriometry signals (Li et al., 2009; Hughes et al., 2009).

4. Acquiring motion data

This section summarises the different sources of motion measurements that are used to form the model. Normally this entails the use of some imaging data, although there has been at least one paper that has proposed measuring motion data by means of electromagnetic tracking (Timinger et al., 2004) rather than imaging.

It is important to note the distinction between the data used for *forming* the motion model and that used to *apply* it. Data used to apply the motion model (i.e. surrogate data) was discussed in Section 3. This section discusses sources of measurements of the true respiratory motion that are used, typically together with the surrogate data, to determine the correspondence model. Section 5.2

Table 5
A summary of the means for acquiring motion data for forming respiratory motion models: CT and MR.

Imaging modality/ measuring device	Details	Examples
MR	Navigator echo	Nehrke et al., 2001
	Breath-hold images	Wang et al., 1995; Blackall et al., 2001; King et al., 2001; Manke et al., 2002b; McLeish et al., 2002; Blackall et al., 2005; Blackall et al., 2006; Reyes et al., 2007
	Respiratory gated images	Manke et al., 2002a; Ablitt et al., 2004; Wu et al., 2006; Buerger et al., 2012; Preiswerk et al., 2012
	Dynamic images	Manke et al., 2003; Khamene et al., 2004; Koch et al., 2004; Liu et al., 2004; Sundaram et al., 2004; Jahnke et al., 2005; Nehrke and Bornert, 2005; Plathow et al., 2005; Blackall et al., 2006; Fischer et al., 2006; Jahnke et al., 2007; Sharif and Bresler, 2007; Gao et al., 2008; King et al., 2008a; King et al., 2008b; King et al., 2009a; King et al., 2009b; White et al., 2009; King et al., 2010b; King et al., 2010c; Rijkhorst et al., 2010; King et al., 2011; McGlashan and King, 2011; Rijkhorst et al., 2011; Savill et al., 2011; King et al., 2012; Peressutti et al., 2012
	k-Space data	Odille et al., 2008b; Odille et al., 2008a; Odille et al., 2010; Filipovic et al., 2011
CT	4-D CT	Li et al., 2006b; Li et al., 2006a; Beddar et al., 2007; Zhang et al., 2007; Ehrhardt et al., 2008; Fayad et al., 2009c; Fayad et al., 2009b; Fayad et al., 2009a; Klinder et al., 2009; McQuaid et al., 2009; Rit et al., 2009; Vandemeulebroucke et al., 2009; Ehrhardt et al., 2010; Fayad et al., 2010; He et al., 2010; Klinder et al., 2010; Liu et al., 2010; Zhang et al., 2010; Ehrhardt et al., 2011; Fayad et al., 2011; Li et al., 2011a; Li et al., 2011b; McQuaid and Lambrou, 2011; Vandemeulebroucke et al., 2011; Klinder and Lorenz, 2012
	4-D Cone Beam CT (CBCT)	Buliev et al., 2003
	Cine CT	Low et al., 2005; McClelland et al., 2005; Chi et al., 2006; McClelland et al., 2006; Ehrhardt et al., 2007; McClelland et al., 2007; Colgan et al., 2008; Yang et al., 2008; Hinkle et al., 2009; Zhao et al., 2009; Low et al., 2010; Geneser et al., 2011; McClelland et al., 2011

Table 6
A summary of the means for acquiring motion data for forming respiratory motion models: X-ray, PET/SPECT, US and miscellaneous.

Imaging modality/ measuring device	Details	Examples
X-ray	Single view, fixed (i.e. fluoroscopy)	*With implanted markers:* Isaksson et al., 2005; Cho et al., 2008; Cho et al., 2010; Cho et al., 2011
		Without implanted markers: Vedam et al., 2003; Ahn et al., 2004; Hoisak et al., 2004; Meyer et al., 2006; Cervino et al., 2009; Cervino et al., 2010
	Single view, rotating (i.e. CBCT projections)	*With implanted markers:* Cho et al., 2010
		Without implanted markers: Martin et al., 2012
	Two views, fixed	*With implanted markers:* Schweikard et al., 2000; Schweikard et al., 2004a; Berbeco et al., 2005; Ionascu et al., 2007; Seppenwoolde et al., 2007; Cho et al., 2008; Ruan et al., 2008; Ernst et al., 2009; Hoogeman et al., 2009; Cho et al., 2010; Torshabi et al., 2010; Cho et al., 2011
		Without implanted markers: Schweikard et al., 2004b; Shechter et al., 2004; Schweikard et al., 2005; Shechter et al., 2005; Shechter et al., 2006; Schneider et al., 2010
PET/SPECT		Klein et al., 2001; Ambwani et al., 2011
US		Atkinson et al., 2001; Ernst et al., 2011
Miscellaneous	Electromagnetic tracking	Timinger et al., 2004
	From 4-D XCAT phantom	Rahni et al., 2011

discusses ways of measuring and representing the motion from these data sources.

Tables 5 and 6 summarise the main sources of motion data that have been proposed in the literature. As can be seen, the main imaging modalities proposed to date have been MR, CT and X-ray. In the table, each of these are broken down further according to the details of the type of imaging data used. These details are important because they can have an influence on the type of motion that the model can capture/estimate. For example, it is now well known that motion states encountered during free-breathing are different from those encountered during breath-hold (e.g. Blackall et al., 2006), so models formed from breath-hold data will have limited accuracy if applied during free-breathing situations. In MR, the first motion model formed from free-breathing (gated) images was Manke et al. (2002a), whereas the first use of dynamic images (i.e. acquired in approximately half a second) was described by Manke et al. (2003).

The use of projection data such as X-ray fluoroscopy or CBCT projections also has significant implications. The use of a single projection limits the dimensionality of the resulting motion data to in-plane motions. The use of two or multiple projections typically necessitates the use of a reconstruction technique to estimate the 3-D motion. Alternatively the multiple 2-D projections can be registered with a 3-D representation of the anatomy, such as a coronary artery segmentation (Schneider et al., 2010).

Due to the noisy nature of the data, long acquisition times and the relatively poor spatial resolution there have been few approaches to using PET or single photon emission computed tomography (SPECT) images alone to make motion measurements for motion models. In addition, it has been common to acquire PET/SPECT data using a gated approach, so to motion-correct a gated PET image a continuous estimate of the motion is not required. Therefore this is not strictly a motion model as defined in Section 1.1. One approach has been to tackle the problem of noisy data by using a motion model to constrain registrations between different respiratory-gated PET images (Ambwani et al., 2011; Klein et al., 2001).

US data is generally relatively poor quality when compared to CT or MR, but can often be acquired with high temporal resolution during an intervention. Therefore US data is rarely used as a source of motion data for building a motion model (Atkinson et al., 2001; Ernst et al., 2011), but has been proposed as surrogate data for driving motion models (Blackall et al., 2005; King et al., 2008b, 2010b; Rijkhorst et al., 2010; Xu and Hamilton, 2006).

5. Models

There are four components that make up a motion model:

- Choice of surrogate data, i.e. **s** in Eqs. (1)–(3): what signals are the input to the model?
- Choice of motion representation: what is the internal representation of the motion in the model? E.g. affine transformation coefficients, control point displacements, etc.
- Correspondence model: how is the motion representation related to the surrogate signals (i.e. ϕ in Eqs. (1)–(3))? How is this relationship parameterised?
- Fitting method: how is the correspondence model fitted to the training data? (i.e. how is ϕ determined?)

Between them, these components will determine the capabilities of the motion model. The different components are interrelated. For example, in order to capture intra-cycle variation (different motion paths during inhalation and exhalation) the following requirements exist: a surrogate signal that can distinguish between inhalation and exhalation; motion data that samples both inhalation and exhalation; a correspondence model that allows different motion estimates for inhalation and exhalation; and an appropriate fitting method.

This section will review the different choices that have been used for each component in the literature, and the implications that the different choices have on the motion models and their capabilities.

5.1. Input signal(s)

Section 3 reviewed different ways in which surrogate signals can be acquired. This section reviews different types of signals (including derived signals) and the implications of these on the motion models. Different physical signals may have stronger or weaker relationships with the respiratory motion. For example, respiratory motion has been found to better correlate with spirometry than with the displacement of a point on the skin surface (Hoisak et al., 2004; Lu et al., 2005). This will affect the accuracy of the motion estimates, but it does not affect the type of motion and variation that can be modelled.

For direct correspondence models (see Section 5.3.1) the type of motion and variation that can be modelled depends on the number

Table 7
A summary of the types of surrogate signals used for direct correspondence models.

Type of surrogate signal(s)	Examples
Single signal	Wang et al., 1995; Schweikard et al., 2000; Atkinson et al., 2001; King et al., 2001; Nehrke et al., 2001; Buliev et al., 2003; Vedam et al., 2003; Ahn et al., 2004; Hoisak et al., 2004; Koch et al., 2004; Liu et al., 2004; Schweikard et al., 2004a; Schweikard et al., 2004b; Blackall et al., 2005; Nehrke and Bornert, 2005; Plathow et al., 2005; Schweikard et al., 2005; Chi et al., 2006; Meyer et al., 2006; Beddar et al., 2007; Ehrhardt et al., 2007; Ionascu et al., 2007; Seppenwoolde et al., 2007; Cho et al., 2008; King et al., 2008b; Ruan et al., 2008; Cervino et al., 2009; Hinkle et al., 2009; Hoogeman et al., 2009; White et al., 2009; Cervino et al., 2010; Cho et al., 2010; King et al., 2010b; King et al., 2010c; King et al., 2010a; Fayad et al., 2011; Geneser et al., 2011; Rijkhorst et al., 2011; Buerger et al., 2012
Respiratory phase	Shechter et al., 2004; McClelland et al., 2005; Shechter et al., 2005; McClelland et al., 2006; Shechter et al., 2006; McClelland et al., 2007; Colgan et al., 2008; Rit et al., 2009; Rijkhorst et al., 2010; McClelland et al., 2011
Single signal and binary signal to distinguish inhalation and exhalation	Blackall et al., 2006; Seppenwoolde et al., 2007; King et al., 2008a; Ernst et al., 2009; Hoogeman et al., 2009; King et al., 2009a; King et al., 2009b; Ernst et al., 2011; King et al., 2011; McClelland et al., 2011; McGlashan and King, 2011; Savill et al., 2011
Single signal + precursor	Manke et al., 2003; Nehrke and Bornert, 2005; Fischer et al., 2006; Zhang et al., 2007; Ruan et al., 2008; Zhang et al., 2010; Cho et al., 2011
	Multiple precursors: Isaksson et al., 2005; Cervino et al., 2009; Cervino et al., 2010
Single signal + gradient	Low et al., 2005; Odille et al., 2008b; Yang et al., 2008; Zhao et al., 2009; Low et al., 2010; McClelland et al., 2011; Martin et al., 2012
Single signal + amplitude	King et al., 2009b
Single signal + respiratory phase	Fayad et al., 2009c
Multiple signals	Manke et al., 2003; Ablitt et al., 2004; Jahnke et al., 2005; Nehrke and Bornert, 2005; Meyer et al., 2006; Wu et al., 2006; Jahnke et al., 2007; Ernst et al., 2009; Fayad et al., 2009b; Fayad et al., 2009a; Klinder et al., 2009; Fayad et al., 2010; He et al., 2010; Klinder et al., 2010; Liu et al., 2010; Torshabi et al., 2010; Ernst et al., 2011; Li et al., 2011b; McGlashan and King, 2011; Rahni et al., 2011; Savill et al., 2011; Klinder and Lorenz, 2012; Preiswerk et al., 2012
Multiple signals + precursors	Torshabi et al., 2010
Multiple signals + gradients	Khamene et al., 2004; Gao et al., 2008; Odille et al., 2008b; Ernst et al., 2009; Ernst et al., 2011

and type of surrogate signals used, as well as the choice of correspondence model. For indirect correspondence models (see Section 5.3.2) the internal variables that parameterise the model determine what type of motion and variation can be modelled. However, it is still important to use appropriate surrogate data. If the images used as surrogates look very similar during inhalation and exhalation then the model will not be able to accurately estimate intra-cycle variation, even if the correspondence model is parameterised in a way that can differentiate between inhalation and exhalation.

Table 7 summarises the types of surrogate signal that have been used with direct correspondence models. We now discuss the implications of the choice between these different approaches. Fig. 3 illustrates the different types of motion trajectories that are possible when relating the motion to different types of surrogate signal. Fig. 3a shows a scalar surrogate signal acquired over approximately two breathing cycles. The points corresponding to end-exhalation (EE 1 and EE 2), mid-inhalation (MI), end-inhalation (EI 1 and EI 2), and mid-exhalation (ME) are marked. Fig. 3b–d are representations of the path the estimated motion could follow in patient space over the two breathing cycles shown in Fig. 3a. When the first breath is inhaled the estimated motion moves from EE 1, through MI, to EI 1. When this breath is exhaled the estimated motion then moves through ME to EE 2. During inhalation of the second breath the estimated motion moves from EE 2 to EI 2.

Fig. 3b shows an example of the type of trajectory that is possible if the motion is just related to the original signal value (the first row of Table 7). As can be seen, the motion is constrained to follow the same trajectory during every breath. It is not possible to distinguish between inhalation and exhalation with just a single signal so no intra-cycle variation can be modelled, i.e. the motion estimate at MI is the same as at ME. A very limited amount of inter-cycle variation can be modelled as the motion estimate can move a different distance along the trajectory from breath to breath, depending on the depth of breathing. A key paper in the use of single scalar surrogate signals is Wang et al. (1995), who first proposed a simple linear model for MR imaging based on diaphragm translation.

Respiratory phase can be used to model intra-cycle variation. Respiratory phase is based on the assumption that breathing is approximately periodic. The surrogate signal is pre-processed so as to parameterise each respiratory cycle between 0% and 100% (with 0% and 100% corresponding to the same respiratory state, often end-exhalation). There are a number of different ways to calculate respiratory phase, depending on whether it needs to be estimated 'on-the-fly' (Ruan et al., 2009) or can be calculated after acquiring the signal for the entire respiratory cycle (McClelland et al., 2011). As can be seen in Fig. 3c using respiratory phase as the surrogate signal constrains the motion to follow the same loop-shaped trajectory during every respiratory cycle. This means that the motion estimate at MI differs from that at ME, so intra-cycle variation can be modelled, but the motion estimates at EE 1 and EI 1 are the same as those at EE 2 and EI 2, so no inter-cycle variation can be modelled. Motion models using respiratory phase were first proposed in Shechter et al. (2004).

Another way to model intra-cycle variation is to distinguish between data acquired during inhalation and exhalation, and to build a separate correspondence model for each set of data (this can be thought of as using an additional binary surrogate signal which differentiates between inhalation and exhalation). This was first proposed in (Blackall et al., 2006), but has since been adopted by many others as can be seen in the third row of Table 7. This enables intra-cycle variation to be modelled as the motion can follow a different trajectory during inhalation than during exhalation, and again allows for limited inter-cycle variation to be modelled as the motion can move a different distance along each trajectory during different breaths. However, the motion may exhibit discontinuous jumps as it switches from the inhalation model to the exhalation model and back again, as illustrated at EI 2 in Fig. 3d. Correspondence models have been developed that constrain the inhalation and exhalation trajectories to meet at either end in the regions corresponding to end-inhalation and end-exhalation (and see Section 5.3.1 Ernst et al., 2009, 2011; King et al., 2009a, 2011), but as long as some of the inhalation and exhalation trajectories differ from each other there will be the possibility of discontinuous jumps in the estimated motion.

In order to model both intra-cycle variation and more complex inter-cycle variation it is necessary to use multiple signals. These could be a single physically measured signal and an extra derived
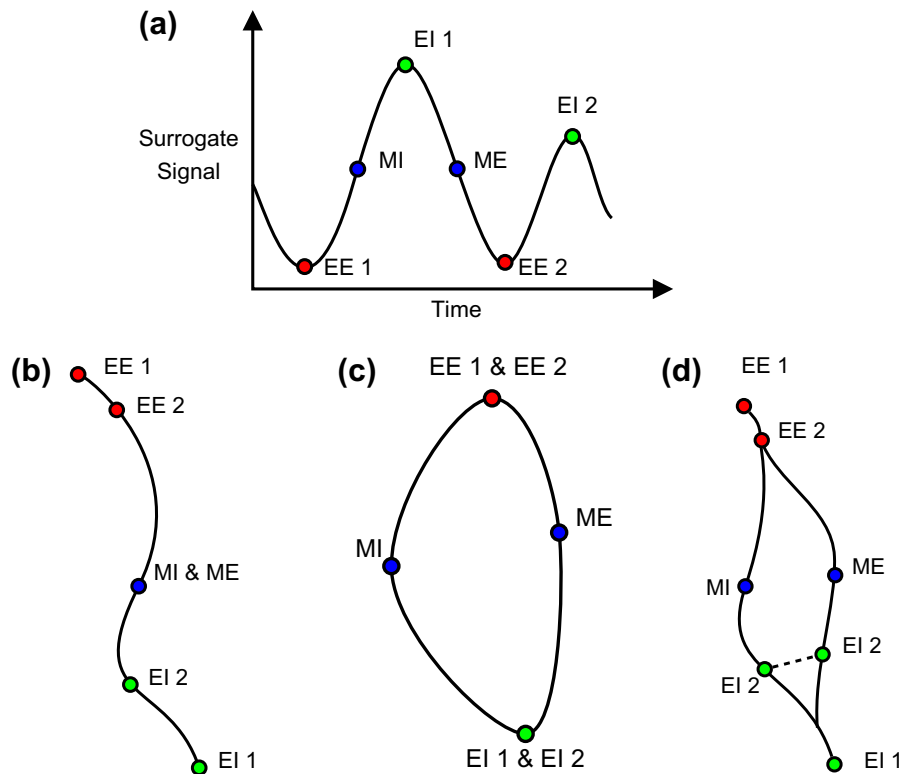
Fig. 3. An illustration of the different types of motion trajectories that are possible when relating the motion to (b) just the original signal value, (c) the respiratory phase, or (d) the original signal value but modelling inhalation and exhalation separately. (a) shows a scalar surrogate signal acquired over approximately two breathing cycles. The points corresponding to end-exhalation (EE 1 and EE 2), mid-inhalation (MI), end-inhalation (EI 1 and EI 2), and mid-exhalation (ME) are annotated. (b–d) are representations of the path the estimated motion could follow in patient space over the two breathing cycles shown in (a).

signal(s) (rows 4 to 7 of Table 7). A popular approach has been to use both the current value of the signal and a *precursor* (i.e. a time-lagged value of the signal), as first proposed in Manke et al. (2003). This idea has also been extended to use multiple precursor values (Cervino et al., 2009, 2010; Isaksson et al., 2005). An alternative but similar idea is to use the gradient (time derivative) of the signal as well as the actual value of the signal, as first proposed in Low et al. (2005). There have also been models proposed that use the value of the signal and an estimate of the amplitude of the signal (the difference between the values at end-exhalation and end-inhalation) (King et al., 2009b), or the value of the signal and the respiratory phase (Fayad et al., 2009c), to enable intra- and inter-cycle variation to be modelled.

Alternatively multiple physical signals could be used (rows 8–10 of Table 7). The first paper to propose this approach was Manke et al. (2003). The different signals typically correspond to the displacement of different parts of the anatomy. In some papers the signals are a subset of the motion data (Klinder and Lorenz, 2012; Preiswerk et al., 2012). Using multiple physical signals can enable the modelling of both intra- and inter-cycle variation. How well different types of variation can be modelled will depend on the nature of the signals used and the relationship between them. For example, using a signal corresponding to chest displacement and another corresponding to abdomen displacement may enable the modelling of the variations between thoracic and abdominal breathing (Odille et al., 2008a). It has also been proposed to use multiple physical signals with derived signals, such as precursors (Torshabi et al., 2010), gradients (Gao et al., 2008; Khamene et al., 2004; Odille et al., 2008b), or even the first and second derivatives of all the signals and a binary signal distinguishing inhalation from exhalation (Ernst et al., 2009, 2011). In general, the more signals used the more variation that can potentially be mod-

elled (depending on how strongly related the different signals are). However, this also relies on using appropriate correspondence models to parameterise the desired variation (see Section 5.3). Also, using more signals exposes the model to "the curse of dimensionality": the more signals and degrees of freedom that the motion models have, the more data is required to fit the correspondence model and the greater the danger of over-fitting (see Section 5.4).

5.2. Motion data

Section 4 described the different ways that data has been acquired in order to measure the motion. This section discusses the different methods used to actually determine the motion from the acquired data, the different ways the motion data has been represented in the motion models, and the amount of variation included in the data used to build and validate the motion models.

The motion has been measured from the imaging data in a number of different ways, as summarised in Table 8. If the motion of only a small number of features (structures or regions) is being modelled, the simplest but most laborious way to determine the motion is to manually delineate the required feature(s) in all of the imaging data. Automatic methods for tracking features of interest have also been proposed, some of which require manual (Manke et al., 2002b) or semi-automatic (Shechter et al., 2004) delineation of the features in one of the images before automatically tracking them in the rest of the images. Sometimes, the features are delineated in 3-D data (e.g. a CT scan) but tracked in 2-D data (e.g. X-ray projections) by simulating projections from the 3-D data (Schneider et al., 2010; Schweikard et al., 2004b, 2005). Implanted markers have also been used as these can be easier to automatically detect and track in the imaging data

Table 8
Summary of the different methods used to measure respiratory motion prior to forming a motion model.

Method of measuring motion	Examples
Manual feature tracking	Wang et al., 1995; Atkinson et al., 2001; Hoisak et al., 2004; Cervino et al., 2009; Cervino et al., 2010; Fayad et al., 2011
Automatic feature tracking	Nehrke et al., 2001; Manke et al., 2002b; Manke et al., 2002a; Buliev et al., 2003; Vedam et al., 2003; Khamene et al., 2004; Koch et al., 2004; Liu et al., 2004; Schweikard et al., 2004b; Shechter et al., 2004; Low et al., 2005; Plathow et al., 2005; Schweikard et al., 2005; Shechter et al., 2005; Chi et al., 2006; Meyer et al., 2006; Shechter et al., 2006; Zhao et al., 2009; Low et al., 2010; Schneider et al., 2010; Ernst et al., 2011 *Using implanted markers:* Schweikard et al., 2000; Schweikard et al., 2004a; Timinger et al., 2004; Berbeco et al., 2005; Isaksson et al., 2005; Beddar et al., 2007; Ionascu et al., 2007; Seppenwoolde et al., 2007; Cho et al., 2008; Ruan et al., 2008; Ernst et al., 2009; Hoogeman et al., 2009; Cho et al., 2010; Torshabi et al., 2010; Cho et al., 2011
Affine registration	Manke et al., 2003; Jahnke et al., 2005; Nehrke and Bornert, 2005; Blackall et al., 2006; Fischer et al., 2006; Jahnke et al., 2007; Reyes et al., 2007; King et al., 2008a; King et al., 2008b; King et al., 2009a; King et al., 2009b; King et al., 2010b; King et al., 2010c; King et al., 2010a; McGlashan and King, 2011; Savill et al., 2011
Deformable registration	Ablitt et al., 2004; Sundaram et al., 2004; Blackall et al., 2005; McClelland et al., 2005; McClelland et al., 2006; Ehrhardt et al., 2007; McClelland et al., 2007; Zhang et al., 2007; Colgan et al., 2008; Yang et al., 2008; Fayad et al., 2009c; Fayad et al., 2009b; Fayad et al., 2009a; Klinder et al., 2009; Rit et al., 2009; Vandemeulebroucke et al., 2009; White et al., 2009; Fayad et al., 2010; He et al., 2010; Klinder et al., 2010; Liu et al., 2010; Zhang et al., 2010; King et al., 2011; Li et al., 2011a; Li et al., 2011b; McClelland et al., 2011; Rahni et al., 2011; Rijkhorst et al., 2011; King et al., 2012; Klinder and Lorenz, 2012; Preiswerk et al., 2012 *Using temporal smoothness cost term:* Klein et al., 2001; Blume et al., 2010; Ambwani et al., 2011 *Using 4-D transformations:* Zeng et al., 2007; Schreibmann et al., 2008; Hinkle et al., 2009; Castillo et al., 2010; King et al., 2010a; Geneser et al., 2011; Metz et al., 2011; Vandemeulebroucke et al., 2011

Table 9
A summary of the representations of the internal motion used for respiratory motion models.

Representation of motion	Examples
Coordinate list	
Points of interest	Schweikard et al., 2000; Ahn et al., 2004; Hoisak et al., 2004; Khamene et al., 2004; Koch et al., 2004; Liu et al., 2004; Schweikard et al., 2004a; Schweikard et al., 2004b; Shechter et al., 2004; Isaksson et al., 2005; Low et al., 2005; Schweikard et al., 2005; Shechter et al., 2005; Chi et al., 2006; Meyer et al., 2006; Shechter et al., 2006; Beddar et al., 2007; Ionascu et al., 2007; Seppenwoolde et al., 2007; Cho et al., 2008; Ruan et al., 2008; Cervino et al., 2009; Ernst et al., 2009; Hoogeman et al., 2009; Zhao et al., 2009; Cervino et al., 2010; Cho et al., 2010; Low et al., 2010; Schneider et al., 2010; Torshabi et al., 2010; Cho et al., 2011; Ernst et al., 2011
Describing a surface	Atkinson et al., 2001; King et al., 2001; Blackall et al., 2006; Klinder et al., 2009; He et al., 2010; Klinder et al., 2010
Rigid/affine transform	
Parameters	Buliev et al., 2003; King et al., 2008b; King et al., 2008a; King et al., 2009a; King et al., 2009b; King et al., 2010a; King et al., 2010b; King et al., 2010c; McGlashan and King, 2011; Rahni et al., 2011; Savill et al., 2011; Martin et al., 2012; Peressutti et al., 2012
Matrix coefficients	Manke et al., 2002a; Manke et al., 2002b; Manke et al., 2003; Jahnke et al., 2005; Nehrke and Bornert, 2005; Fischer et al., 2006; Jahnke et al., 2007
Deformable transform	
Deformation field	Sundaram et al., 2004; Li et al., 2006b; Li et al., 2006a; Zhang et al., 2007; Ehrhardt et al., 2007; Ehrhardt et al., 2008; Yang et al., 2008; Fayad et al., 2009c; Fayad et al., 2009b; Fayad et al., 2009a; Rit et al., 2009; Vandemeulebroucke et al., 2009; White et al., 2009; Fayad et al., 2010; Liu et al., 2010; Zhang et al., 2010; Li et al., 2011a; Li et al., 2011b; Rijkhorst et al., 2011; Klinder and Lorenz, 2012; Preiswerk et al., 2012
Velocity field	Hinkle et al., 2009; Ehrhardt et al., 2010; Ehrhardt et al., 2011; Geneser et al., 2011
B-spline control point grid	Ablitt et al., 2004; Blackall et al., 2005; McClelland et al., 2005; McClelland et al., 2006; McClelland et al., 2007; Colgan et al., 2008; Gao et al., 2008; King et al., 2011; McClelland et al., 2011; Buerger et al., 2012; King et al., 2012

(especially for X-ray projection data). Magnetic tracking systems have also been used which automatically measure the motion of a marker without actually requiring any imaging data (Timinger et al., 2004).

For modelling the motion of large regions of interest image registration techniques have commonly been used to measure the motion. For some applications, e.g. when modelling the respiratory motion of the heart, an affine registration is sufficient to approximate the motion of the region of interest. For other applications, e.g. modelling the deformation of the lungs due to breathing, a deformable registration is required. Many different deformable registration algorithms have been utilised for motion models, e.g. B-spline (McClelland et al., 2006; Rueckert et al., 1999), demons (Li et al., 2011a; Thirion, 1998), optical flow/diffusion (Horn and Schunck, 1981; Zhang et al., 2007), fluid (Christensen et al., 1996; Liu et al., 2010), locally affine (Buerger et al., 2011; King et al., 2011), etc. A description of the different algorithms and a discussion of their advantages and disadvantages is beyond the scope of this paper, but a number of good review papers or comparative studies of deformable registration have previously been published, e.g. Brock (2010), Makela et al. (2002), Murphy et al. (2011).

Image registration is usually performed on each image individually, but some methods simultaneously register all of the images in order to exploit the temporal nature of the data. One way in which this has been done is to maintain a separate transformation for each image, but to include a temporal smoothness cost term which penalises transformations that do not change smoothly in time (Ambwani et al., 2011; Blume et al., 2010; Klein et al., 2001). Another way is to extend the transformation model to the temporal dimension, i.e. rather than using a series of 3-D transformations, use a single 4-D transformation and fit this transformation to all of the image data simultaneously (Castillo et al., 2010; Geneser et al., 2011; Hinkle et al., 2009; King et al., 2010a; Metz et al., 2011; Schreibmann et al., 2008; Vandemeulebroucke et al., 2011; Zeng et al., 2007). The transformation can either represent the temporal dimension using the same model as the spatial dimensions, e.g. a 4-D B-spline transformation (Zeng et al., 2007), or it can use a different model for the spatial and temporal dimensions, e.g. an affine transformation for the spatial dimensions and a polynomial for the temporal dimensions (King et al., 2010a).

The way that the motion is represented in the correspondence model usually, but not always, depends on how the motion has been measured. Table 9 summarises the different ways in which the motion has been represented.

To build a motion model the motion is sampled a number of times, and these samples are used to fit the correspondence model

(see Sections 5.3 and 5.4). Usually, each sample is a list of coordinates or a transformation representing the motion at a specific point in time (or a specific point in the respiratory cycle if using gated data, see Section 4). The correspondence model can then estimate what the motion is at a new point in time from the surrogate signal(s). In contrast, some models use samples that correspond to entire breathing cycles rather than specific points in time (Ehrhardt et al., 2008, 2010; Fayad et al., 2009a, 2010; Klinder et al., 2009, 2010). This means that the correspondence model will estimate the motion for a whole breathing cycle (and will also require the surrogate signal values corresponding to a whole breathing cycle) rather than for a single point in time. In this case the correspondence model does not describe the relationship between the surrogate signal(s) and the respiratory motion, but describes the relationship between the inter-cycle variation of the surrogate signal(s) and the inter-cycle variation of the respiratory motion.

The data used to fit the models can sample different types of variation in the motion (see Section 1.2), as shown in Table 10. Some works have used either breath-hold data or data acquired during inhalation or exhalation from a single breathing cycle, so do not sample any types of variation. Other works have used data from an entire breathing cycle, and therefore sample intra-cycle variation, but as the data comes from only a single cycle they do not sample inter-cycle variation. The first paper to use data sampling intra-cycle variation was Schweikert et al. (2000), but it is now common practice to sample intra-cycle variation as motion estimates are usually required for both inhalation and exhalation (note, references in the lower rows of Table 10 also sample intra-cycle variation). *Respiratory sorted data* (sometimes referred to as respiratory correlated data in the literature) has also been used, such as gated MR (Ablitt et al., 2004; Buerger et al., 2012) or 4-D CT, e.g. Zhang et al. (2007). Data is acquired over several breathing cycles but only partial data is acquired during each cycle. A surrogate signal is then used to bin the data to form coherent volumes. These data represent a single breathing cycle so do not sample inter-cycle variation. Any inter-cycle variation that occurs during acquisition will cause artefacts in the images. Usually, the sorted volumes distinguish between inhale and exhale (e.g. by sorting them according to respiratory phase) so sample intra-cycle variation.

Some papers have used data acquired over multiple respiratory cycles, which therefore sample inter-cycle variation. Schweikard et al. (2000) was the first to use data from multiple respiratory cycles, although many other papers have also sampled inter-cycle variation as can be seen from Table 10. Sometimes, the subjects are asked to breathe in different ways (e.g. deep/shallow, abdominal/thoracic) during data acquisition, in order to explicitly sample such variations. Koch et al. (2004), Liu et al. (2004), and Plathow et al. (2005) investigated how different types of breathing could affect simple linear correlations between a surrogate signal and the respiratory motion. In King et al. (2009b) a method of modelling the different types of respiratory motion and combining them to form a single motion estimate was proposed. Some papers have used data acquired over several weeks of RT treatment in order to sample inter-fraction variations (Klinder et al., 2009, 2010). Other works have used data from different patients, and attempted to build a generic population based model that can model inter-subject variation. Population based models were first proposed in Sundaram et al. (2004), but have been most thoroughly developed in Ehrhardt et al. (2011).

It should be emphasised that it is the combination of surrogate signals and correspondence model that determines the types of variation that can be modelled. The data used to fit the model usually samples the different types of variation that are to be modelled. However, it is possible to build a model that can estimate how the motion varies without actually sampling the variation. For example, in Fayad et al. (2009c) and Zhang et al. (2007) models were built that could potentially model inter-cycle variation, but the models were formed using data from a 4-D CT dataset representing a single breathing cycle. In these cases it is assumed that the relationship between the motion and the surrogate signals can be inferred from a limited amount of data, and that the relationship is robust enough that it can be extrapolated to estimate the motion outside of the range used to fit the model. Although such models may be appealing from a clinical perspective as they require less data to build them, it is impossible to know how accurately the motion can be extrapolated and over what range.

Finally, some papers have described models representing different types of motion and then used the models to study how the motion varied in different circumstances, e.g. intra-cycle variation (Blackall et al., 2006), inter-cycle variation (Blackall et al., 2006), breath-hold vs free-breathing (Blackall et al., 2006), deep breathing vs normal breathing vs shallow breathing (King et al., 2008a, 2012), and inter-fraction variation (McClelland et al., 2011).

5.3. Correspondence models

The correspondence model defines the relationship between the surrogate signals and the respiratory motion. As noted in Section 1.1.1 there are two types of correspondence model: direct correspondence models and indirect correspondence models.

Table 10
Summary of the different types of variation sampled by the motion data used to build the models.

Type of variation	Examples
None	King et al., 2001; Blackall et al., 2005; Blackall et al., 2006; Reyes et al., 2007
Intra-cycle variation	Shechter et al., 2004; Shechter et al., 2005; Chi et al., 2006; Shechter et al., 2006; Beddar et al., 2007; Hinkle et al., 2009; Geneser et al., 2011; Rahni et al., 2011
	Using respiratory sorted data: Buliev et al., 2003; Ablitt et al., 2004; Zhang et al., 2007; Fayad et al., 2009c; Fayad et al., 2009b; Rit et al., 2009; Vandemeulebroucke et al., 2009; Liu et al., 2010; Zhang et al., 2010; Fayad et al., 2011; Li et al., 2011a; Li et al., 2011b; Buerger et al., 2012
Inter-cycle variation	Schweikard et al., 2000; Manke et al., 2002a; Manke et al., 2002b; Manke et al., 2003; Ahn et al., 2004; Hoisak et al., 2004; Schweikard et al., 2004a; Schweikard et al., 2004b; Berbeco et al., 2005; Isaksson et al., 2005; Jahnke et al., 2005; Low et al., 2005; McClelland et al., 2005; Nehrke and Bornert, 2005; Schweikard et al., 2005; Fischer et al., 2006; McClelland et al., 2006; Meyer et al., 2006; Ehrhardt et al., 2007; Ionascu et al., 2007; Jahnke et al., 2007; McClelland et al., 2007; Seppenwoolde et al., 2007; Cho et al., 2008; Colgan et al., 2008; Gao et al., 2008; Ruan et al., 2008; Yang et al., 2008; Zhao et al., 2009; Cervino et al., 2009; White et al., 2009; Hoogeman et al., 2009; Ernst et al., 2009; King et al., 2009a; King et al., 2010a; King et al., 2010c; Cervino et al., 2010; Cho et al., 2010; Low et al., 2010; Torshabi et al., 2010; Cho et al., 2011; Ernst et al., 2011; McClelland et al., 2011; Rijkhorst et al., 2011; Martin et al., 2012; Preiswerk et al., 2012
	Including different types of breathing: Koch et al., 2004; Liu et al., 2004; Plathow et al., 2005; King et al., 2008a; King et al., 2008b; King et al., 2009b; King et al., 2010b; King et al., 2011; McGlashan and King, 2011; Savill et al., 2011; King et al., 2012; Peressutti et al., 2012
Inter-fraction variation	Klinder et al., 2009; Klinder et al., 2010
Inter-patient variation	Sundaram et al., 2004; Ehrhardt et al., 2008; Fayad et al., 2009a; Klinder et al., 2009; Ehrhardt et al., 2010; Fayad et al., 2010; He et al., 2010; Ehrhardt et al., 2011; Klinder and Lorenz, 2012; Preiswerk et al., 2012

Table 11
Summary of the different types of direct correspondence models used in the literature: linear and piecewise linear.

Type	Details	Examples
Linear	1 surrogate signal	Wang et al., 1995; Schweikard et al., 2000; Atkinson et al., 2001; Nehrke et al., 2001; Manke et al., 2002a; Manke et al., 2002b; Buliev et al., 2003; Ahn et al., 2004; Hoisak et al., 2004; Koch et al., 2004; Liu et al., 2004; Schweikard et al., 2004a; Schweikard et al., 2004b; Timinger et al., 2004; Plathow et al., 2005; Schweikard et al., 2005; Chi et al., 2006; Beddar et al., 2007; Ionascu et al., 2007; Seppenwoolde et al., 2007; Cho et al., 2008; Ruan et al., 2008; Cervino et al., 2009; Hoogeman et al., 2009; White et al., 2009; Cervino et al., 2010; Cho et al., 2010; Fayad et al., 2011
	2 or more surrogate signals	Manke et al., 2003; Ablitt et al., 2004; Isaksson et al., 2005; Jahnke et al., 2005; Low et al., 2005; Fischer et al., 2006; Meyer et al., 2006; Wu et al., 2006; Jahnke et al., 2007; Sharif and Bresler, 2007; Zhang et al., 2007; Gao et al., 2008; Odille et al., 2008b; Odille et al., 2008a; Ruan et al., 2008; Yang et al., 2008; Cervino et al., 2009; Ernst et al., 2009; Fayad et al., 2009b; Fayad et al., 2009a; Klinder et al., 2009; Zhao et al., 2009; Klinder et al., 2010; Liu et al., 2010; Cervino et al., 2010; Fayad et al., 2010; Low et al., 2010; Zhang et al., 2010; Cho et al., 2011; Ernst et al., 2011; Li et al., 2011b; McClelland et al., 2011; Rahni et al., 2011; Martin et al., 2012; Klinder and Lorenz, 2012; Preiswerk et al., 2012
Piece-wise linear	1 surrogate signal	Ehrhardt et al., 2007; Hinkle et al., 2009; Geneser et al., 2011
	Respiratory phase surrogate signal	Rit et al., 2009

Table 12
Summary of the different types of direct correspondence models used in the literature: polynomial, B-spline and others.

Type	Details	Examples
Polynomial	1 surrogate signal	McClelland et al., 2005; Nehrke and Bornert, 2005; Ruan et al., 2008; Hoogeman et al., 2009; King et al., 2010c; King et al., 2010a; Ernst et al., 2011; Rijkhorst et al., 2011
	1 surrogate signal with separate inhalation and exhalation	Blackall et al., 2006; Seppenwoolde et al., 2007; King et al., 2008a; Ernst et al., 2009; Hoogeman et al., 2009; King et al., 2009a; King et al., 2009b; Torshabi et al., 2010; Ernst et al., 2011; King et al., 2011; McClelland et al., 2011; McGlashan and King, 2011; Savill et al., 2011
	2 surrogate signals	Ruan et al., 2008; Torshabi et al., 2010
B-spline	1 surrogate signal	Buerger et al., 2012
	Respiratory phase surrogate signal and periodic B-splines	Shechter et al., 2004; McClelland et al., 2005; Shechter et al., 2005; McClelland et al., 2006; Shechter et al., 2006; McClelland et al., 2007; Colgan et al., 2008; Rijkhorst et al., 2010; McClelland et al., 2011; Vandemeulebroucke et al., 2011
	2 or more surrogate signals	Khamene et al., 2004; Fayad et al., 2009c
Others	Fourier series	McClelland et al., 2005
	Neural networks	Isaksson et al., 2005; Torshabi et al., 2010
	Fuzzy logic	Torshabi et al., 2010
	Least squares support vector machines	He et al., 2010
	Support vector regression	Ernst et al., 2009; Ernst et al., 2011

5.3.1. Direct correspondence models

A direct correspondence model estimates the motion as a direct function of the surrogate signal(s). There is a close link between the choice of surrogate signals and the choice of correspondence model. For example, Nehrke and Bornert (2005) describe their method as using a quadratic surrogate signal, whilst Seppenwoolde et al. (2007) describe the same approach as using a quadratic correspondence model. The number of (independent) surrogate signals determines the number of degrees of freedom of the model.

A number of different correspondence models have been used in the literature, as can be seen in Tables 11 and 12. The most common is a linear correspondence model, where the motion is modelled as a linear combination of the surrogate signals. Referring back to Eqs. (1)–(3),

$$\phi(\mathbf{s}) = \mathbf{As} + \mathbf{A_0}, \qquad (4)$$

where $\mathbf{s}$ is a vector of surrogate signals, $\mathbf{A}$ is a matrix specifying the linear combination of surrogate values and $\mathbf{A_0}$ is a vector of constants.

Several papers use a linear model with just a single surrogate signal (i.e. $\mathbf{s}$ is a scalar value), which is therefore a simple linear correlation between the surrogate signal and the motion. This constrains the motion to follow a straight line during each breath (i.e. the trajectory in Fig. 3b would be linear). Such a model was first proposed by Wang et al. (1995), and although the model may not be very realistic, it has since been used and investigated by many others. There have been a number of studies assessing how different factors can affect the correlation between the surrogate signal and the motion (Ahn et al., 2004; Beddar et al., 2007; Chi et al., 2006; Fayad et al., 2011; Hoisak et al., 2004; Ionascu et al., 2007; Koch et al., 2004; Liu et al., 2004; Plathow et al., 2005), e.g. the surrogate signal used (Hoisak et al., 2004), the type of breathing the patient is performing (deep or shallow, using their ribs or using their diaphragm) (Koch et al., 2004; Plathow et al., 2005), and over what time scales the linear correlations are valid (Hoisak et al., 2004). These studies have had mixed results. In some circumstances a simple linear correlation can approximate the respiratory motion relatively well over a short time frame, but in other circumstances, such as when there is significant intra-cycle variation, a simple 1-D linear correlation is not sufficient.

Other papers have used linear models of two or more (sometimes many more) surrogate signals. When there are only two signals these usually comprise one measured surrogate signal and either its gradient or a precursor. When more signals are used they are often multiple physical surrogate signals from different parts of the anatomy, although sometimes they will also include derived signals, such as the gradients of the signals. Sometimes the different signals may be highly correlated with each other, e.g. when the signals represent points on the surface of an organ, and this can make the models susceptible to over-fitting (Klinder et al., 2009, 2010). However, the models are very flexible and can potentially model complex motion and both intra- and inter-cycle variation.

Linear models using multiple surrogate signals were first proposed by Manke et al. (2003) for motion correction in MR imaging, and later by Low et al. (2005) for planning and guiding RT treatment.

One way to model more complex motion with only a single surrogate signal is to use a piece-wise linear model (Geneser et al., 2011; Hinkle et al., 2009; Rit et al., 2009). In this case the motion is defined for a number of discrete values of the surrogate signal, e.g. by performing deformable registrations on different images from a 4-D CT dataset. These motion estimates are linearly interpolated to give the motion estimates at other surrogate signal values. Therefore, the trajectory shown in Fig. 3b would be piece-wise linear. Such models allow the motion to follow more complex paths than a simple straight line, but as with any model using a single surrogate signal, they are limited in the variation they can model. Furthermore, a piece-wise linear model cannot extrapolate outside the range of surrogate signal values used to build the model. A piece-wise linear model can also be used with a respiratory phase surrogate signal (Rit et al., 2009), allowing intra-cycle variation to be modelled but not inter-cycle variation.

Polynomial correspondence models have also been widely used. These estimate the motion as a polynomial function of the surrogate signal(s). Referring again to Eqs. (1)–(3), we have

$$\phi(s_1) = \sum_{i=0}^{n} \mathbf{A}_i s_1^i, \tag{5}$$

for a single surrogate signal or

$$\phi(s_1, s_2) = \sum_{i=0}^{n} \sum_{j=0}^{n-i} \mathbf{A}_{i,j} s_1^i s_2^j, \tag{6}$$

for a bivariate model of 2 surrogate signals. s_1 and s_2 are scalar surrogate signals. $\mathbf{A}_i$ and $\mathbf{A}_{i,j}$ are vectors of polynomial coefficients and n is the polynomial order.

Such models are usually 2nd or 3rd order polynomials. Higher orders polynomials have been investigated (McClelland et al., 2005), but they are more likely to over-fit the data and lead to very large extrapolation errors. Polynomial models were first proposed for direct correspondence models in Nehrke and Bornert (2005) and Blackall et al. (2006), but had previously been proposed for indirect correspondence models in King et al. (2001). Polynomial models are usually used with a single scalar surrogate signal, but they have also been used with respiratory phase (McClelland et al., 2005), and with two surrogate signals (the second being a precursor of the first) (Ruan et al., 2008; Torshabi et al., 2010). Separate polynomial models can be fitted to the data from inhalation and exhalation, as first proposed in Blackall et al. (2006). This allows intra-cycle variation to be modelled. As polynomial models can be susceptible to large extrapolation errors some papers revert to using a linear model when estimating the motion for values of the surrogate signal that are outside the range used to build the model (Ernst et al., 2009, 2011; Seppenwoolde et al., 2007; Torshabi et al., 2010). To try and minimise the discontinuities when switching between inhalation and exhalation models the polynomials can be constrained to meet in the regions corresponding to end-inhale and end-exhale (King et al., 2009a, 2011). Other papers 'blend together' the polynomial models and a linear model in the regions corresponding to end-exhale and end-inhale, creating a smooth transition from one model to the other and allowing the linear model to be used when extrapolation is required (Ernst et al., 2009, 2011).

King et al. (2009b) proposed an adaptive correspondence model that could adapt to different types of breathing (e.g. deep breathing or shallow breathing). This work used polynomial models, although the approach could be used with any type of direct correspondence model. Separate sub-models are fitted for each of the different types of breathing. Each sub-model is used to make a motion estimate for the current value of the surrogate signal. The amplitude of the surrogate signal is then used to interpolate between the motion estimates from the different sub-models to give the final motion estimate output by the model.

B-spline correspondence models have also been proposed to relate the surrogate signal(s) and the motion. Most of these techniques use a single surrogate signal so only use a 1-D B-spline, but B-splines of two (Fayad et al., 2009c) or more (Khamene et al., 2004) dimensions have also been proposed for models using multiple surrogate signals. Many of these works use respiratory phase as the surrogate signal, and so modify the B-spline function to make it 'periodic' (or 'cyclic') so that there are no discontinuities between one breathing cycle and the next. Referring to Eqs. (1)–(3), the periodic B-spline model can be written as:

$$\phi(\vartheta) = \sum_{i=0}^{3} B_i(j) c_{i+k \bmod N}, \tag{7}$$

where ϑ is the respiratory phase (between 0% and 100%), B_i is the ith B-spline basis function (see Rueckert et al., 1999), $j = \frac{\vartheta}{\delta} - \lfloor \frac{\vartheta}{\delta} \rfloor, k = \lfloor \frac{\vartheta}{\delta} \rfloor - 1, c_0, \dots c, c_N$ are the values of the B-spline control points, N is the number of control points, and δ is the control point spacing ($\delta = \frac{100\%}{N}$). B-spline correspondence models were first proposed in Khamene et al. (2004), but were fully developed (including being made periodic) in (Shechter et al., 2004) and independently in McClelland et al. (2005, 2006).

Other correspondence models have also been proposed in the literature but have not been widely used, including models based on Fourier series (McClelland et al., 2005), neural networks (Isaksson et al., 2005; Torshabi et al., 2010), fuzzy logic (Torshabi et al., 2010), least squares support vector machines (He et al., 2010), and support vector regression (Ernst et al., 2011, 2009). There have been a few papers comparing different correspondence models (Ernst et al., 2011, 2009; McClelland et al., 2005, 2011; Ruan et al., 2008; Seppenwoolde et al., 2007; Torshabi et al., 2010), but these only compare a small selection of models (with different models used in each paper) on limited data, and so cannot be used to draw general conclusions about the relative performance of different models.

5.3.2. Indirect correspondence models

Indirect correspondence models do not directly relate the motion to the surrogate data. Instead, they parameterise the motion using one or more internal variables, and make estimates of the surrogate data as well as the motion data. When surrogate data is acquired during a procedure the internal variables are optimised to give the best match between the estimated surrogate data and the measured surrogate data. This approach was first proposed in King et al. (2001), but has become more popular in the last few years.

To date, the surrogate data used with indirect correspondence models in the literature has always been some kind of image data, although indirect correspondence models using surfaces or even simple scalar signals as surrogate data could be envisaged. Typically, the appearance of the anatomy corresponding to different values of the internal variables is estimated by transforming a 3-D reference volume (e.g. MR, CT or US). The surrogate data can be compared directly to the transformed reference volume (King et al., 2008b, 2010b; Peressutti et al., 2012) or can be simulated from it. Returning to Eqs. (1)–(3), if the surrogate data is compared directly to the transformed reference volume the function F just selects the part of the reference volume that corresponds to the surrogate data. If the transformed reference volume is used to simulate the modality of the surrogate data then F represents this simulation process. For example, the simulation can consist of

Table 13
Summary of the different types of indirect correspondence models used in the literature.

Type	Examples
1-D linear	White et al., 2009
Multi-D linear	Schneider et al., 2010; Li et al., 2011a; King et al., 2012
Polynomial	King et al., 2001; Blackall et al., 2005; King et al., 2008b; King et al., 2010b; Peressutti et al., 2012
Cyclic B-spline (with linear scaling)	Vandemeulebroucke et al., 2009

Table 14
Summary of the different fitting methods used in the literature.

Type	Examples
Linear least squares	Wang et al., 1995; Schweikard et al., 2000; King et al., 2001; Nehrke et al., 2001; Manke et al., 2002a; Manke et al., 2002b; Buliev et al., 2003; Khamene et al., 2004; Schweikard et al., 2004a; Schweikard et al., 2004b; Shechter et al., 2004; Timinger et al., 2004; Blackall et al., 2005; Isaksson et al., 2005; Low et al., 2005; McClelland et al., 2005; Schweikard et al., 2005; Shechter et al., 2005; Blackall et al., 2006; McClelland et al., 2006; Meyer et al., 2006; Shechter et al., 2006; McClelland et al., 2007; Seppenwoolde et al., 2007; Cho et al., 2008; Colgan et al., 2008; King et al., 2008b; Ruan et al., 2008; Yang et al., 2008; Ernst et al., 2009; Hoogeman et al., 2009; White et al., 2009; Cho et al., 2010; King et al., 2010b; King et al., 2010c; King et al., 2010a; Low et al., 2010; Rijkhorst et al., 2010; Torshabi et al., 2010; Cho et al., 2011; Ernst et al., 2011; King et al., 2011; McClelland et al., 2011; McGlashan and King, 2011; Rijkhorst et al., 2011; Savill et al., 2011; Peressutti et al., 2012
Constrained least squares	King et al., 2008a; King et al., 2009a; King et al., 2009b
Ridge regression	Klinder et al., 2009; He et al., 2010
Principal component regression	Klinder et al., 2010
Partial least squares regression	Ablitt et al., 2004; Wu et al., 2006
Canonical correlation analysis	Gao et al., 2008; Liu et al., 2010
Support vector regression	Ernst et al., 2009; Ernst et al., 2011
Maximum a posterior estimator	Li et al., 2011b
Multi-level B-spline approximation	Fayad et al., 2009c; Buerger et al., 2012
Nelder-Mead optimisation	Zhao et al., 2009
Levenberg–Marquardt algorithm	Isaksson et al., 2005; Torshabi et al., 2010
Fuzzy logic methods	Torshabi et al., 2010
Digital filtering	Vandemeulebroucke et al., 2009
Particle filters	Rahni et al., 2011
4-D registration	Klein et al., 2001; Zeng et al., 2007; Schreibmann et al., 2008; Blume et al., 2010; Castillo et al., 2010; King et al., 2010a; Metz et al., 2011; Vandemeulebroucke et al., 2011
4-D registration combined with motion compensated image reconstruction	Odille et al., 2008b; Odille et al., 2008a; Hinkle et al., 2009; Odille et al., 2010; Ambwani et al., 2011; Filipovic et al., 2011; Geneser et al., 2011; Martin et al., 2012

taking a projection through the volume to simulate an X-ray projection (Li et al., 2011a; Vandemeulebroucke et al., 2009) or processing the volume to simulate US data (Blackall et al., 2005; King et al., 2001, 2010c). The simulated surrogate data is then compared to the measured surrogate data in order to find the optimum values of the internal variables. Fitting the internal variables to surrogate data from an entire breathing cycle simultaneously has been proposed to help provide a more robust fit (Vandemeulebroucke et al., 2009).

In some papers the internal variables used to parameterise the motion correspond to physical surrogate signals (Blackall et al., 2005; King et al., 2008b, 2010b; Vandemeulebroucke et al., 2009; White et al., 2009). However, they are only used to fit the model, and are not directly measured when making estimates with the model. In other papers the internal variables are more abstract, e.g. PCA weights, and do not have direct physical interpretations (Li et al., 2011a; King et al., 2012; Schneider et al., 2010). Similar models have been used for indirect correspondence models as have been used for direct correspondence models, as can be seen in Table 13. The types of motion and variation that can be modelled with these are the same as for the direct correspondence models. A model has also been proposed that relates the motion to respiratory phase using a cyclic B-spline, but allows for some inter-cycle variation by linearly scaling the motion estimate depending on the amplitude of the breathing (Vandemeulebroucke et al., 2009).

Finally, it should be noted that the distinction between direct and indirect correspondence models is not always straightforward. For example, one recent work (Peressutti et al., 2012) has proposed a motion model that uses a combination of a measured surrogate signal (as used with direct correspondence models) and imaging data (as used with indirect correspondence models) to make motion estimates.

5.4. Fitting method

A number of different methods and techniques have been used to fit the correspondence models to the data. As can be seen in Table 14 by far the most commonly used method is linear least squares. Some of the other methods are extensions of linear least squares or are closely related, and can have advantages over standard linear least squares in some circumstances. For example, when modelling inhalation and exhalation using separate correspondence models (i.e. so that intra-cycle variation can be modelled) constrained least squares has been used to ensure that the models meet up at end-inhalation and end-exhalation (King et al., 2008a, 2009a,b). Ridge regression (Klinder et al., 2009; He et al., 2010) and principal components regression (Klinder et al., 2010) are both modifications of linear least squares that help provide a more robust fit to the data. This can be particularly useful if there are a large number of surrogate signals that are highly correlated with each other, e.g. when the surrogate signals are from points on an organ/skin surface, and can help prevent over-fitting in such circumstances. Most of the fitting methods used in the literature are general fitting methods that can be used to fit many different correspondence models, but some are specialised methods designed for specific correspondence models (e.g. multi-level B-spline approximation can only be used to fit B-spline correspondence models).

Table 15
Summary of the different ways PCA has been utilised when fitting motion models in the literature.

PCA applied to:	Examples
Motion data	*Prior to fitting a correspondence model:* King et al., 2001; Gao et al., 2008; Zhang et al., 2010
	To parameterise the motion: Blackall et al., 2001; Schneider et al., 2010; Ehrhardt et al., 2011; Li et al., 2011a; King et al., 2012
Surrogate data	Klinder et al., 2010
Motion data and surrogate data	*Separately:* Khamene et al., 2004; Liu et al., 2010
	Combined: Manke et al., 2003; Jahnke et al., 2005; Nehrke and Bornert, 2005; Fischer et al., 2006; Jahnke et al., 2007; Sharif and Bresler, 2007; Zhang et al., 2007; Cervino et al., 2009; Fayad et al., 2009b; Fayad et al., 2009a; Klinder et al., 2009; Cervino et al., 2010; Fayad et al., 2010; Li et al., 2011b; Klinder and Lorenz, 2012; Preiswerk et al., 2012

As noted in Section 5.2, a 4-D registration can be seen as fitting a correspondence model directly to the image data, i.e. simultaneously estimating the motion and fitting the correspondence model. 4-D registration (for modelling respiratory motion) was first proposed in Klein et al. (2001) for affine transformations and in Zeng et al. (2007) and Schreibmann et al. (2008) for deformable transformations. This approach can also be combined with motion compensated image reconstruction, as first proposed in Odille et al. (2008b) for MR imaging and in Hinkle et al. (2009) for CT imaging. These methods iterate between performing motion compensated image reconstruction (using the current correspondence model and the known surrogate signal values), and fitting the correspondence model directly to the image data (using the current motion compensated reconstruction).

PCA (Jolliffe, 2002) has been utilised in a number of different ways when fitting the motion models, as can be seen in Table 15. It has been applied to the internal motion data prior to fitting a correspondence model. In this case, the correspondence model relates the surrogate signal(s) to the PCA weights which describe the motion. Note, linear least squares or some other fitting method still needs to be used to fit the correspondence model. Using PCA in this way can help remove unwanted noise from the motion data due to imaging and/or registration errors.

PCA has been applied to the motion data as a way to parameterise the motion without directly relating it to the surrogate signals (i.e. no direct correspondence model is fitted to the data). The results of the PCA can then be used for an indirect correspondence model (see Section 5.3.2) (King et al., 2012; Li et al., 2011a; Schneider et al., 2010).

PCA has also been applied to the surrogate signal data before fitting a correspondence model. The correspondence model then relates the PCA weights (which now represent the surrogate signals) to the motion. This approach is known as principal component regression (PCR) and it can help provide a more stable and robust fit by removing co-linearities in the surrogate data.

Another use of PCA has been to apply it to both the motion data and the surrogate data separately, before fitting a correspondence model relating the motion PCA weights to the surrogate data PCA weights (Khamene et al., 2004; Liu et al., 2010). This should both help to remove noise from the motion data and remove co-linearities from the surrogate data. A similar approach, which is more widely used in the literature, is to combine all the surrogate data and internal motion data into a single data vector, and to perform PCA on the combined data vector. The principal components can be split into two matrices (one corresponding to the internal motion data and one to the surrogate data), and a correspondence model can be fitted relating these two matrices. This approach was first proposed by Manke et al. (2003) and has since been adopted by many others.

A number of papers have used an approach that can be termed 'adaptive' fitting (Cho et al., 2008, 2010, 2011; Hoogeman et al., 2009; Isaksson et al., 2005; King et al., 2012; Schweikard et al., 2000; Schweikard et al., 2004a,b, 2005; Seppenwoolde et al., 2007; Torshabi et al., 2010). In this approach the model is initially fit to some training data acquired at the start of the procedure. Then during the procedure further internal motion data is intermittently acquired (together with surrogate data). This data is used to update the model so that it can adapt to gradual changes to the correspondence model. This is usually done by discarding the oldest internal motion sample in favour of the most recent sample, and re-fitting the model. The newly acquired motion data can also be used to check how accurate the current model is. If it is found that the accuracy drops below a certain tolerance, the procedure can be paused while enough imaging data is acquired to completely rebuild the model. This approach can help detect and account for more sudden changes to the correspondence models. This 'adaptive' approach was first proposed in Schweikard et al. (2000) and is used in the commercially available Cyberknife system.[3]

5.5. Cross-population models

A number of papers have proposed methods to generate cross-population models (Ehrhardt et al., 2011, 2010, 2008; Fayad et al., 2009a, 2010; He et al., 2010; Klinder et al., 2009, 2012; Preiswerk et al., 2012; Sundaram et al., 2004). These models are fit to data from different individuals, so can model (or 'average out') inter-subject variation. As respiratory motion can vary dramatically between individuals (Keall et al., 2006), particularly if they have a pathology, it is unlikely that cross-population models will ever be as accurate as subject specific models. In addition, it is very challenging to acquire data from enough subjects to adequately sample the inter-subject variation. However, preliminary studies have shown promising results for cross-population models, and they could potentially be very useful and enable respiratory motion to be estimated without acquiring any motion data from the individual.

Some of the cross-population methods use direct correspondence models to relate the motion to surrogate signals in the same way as for subject specific models (Fayad et al., 2009a, 2010; He et al., 2010; Klinder et al., 2009, 2012; Preiswerk et al., 2012). Other cross-population models do not relate the internal motion to surrogate data (Ehrhardt et al., 2011, 2010, 2008; Sundaram et al., 2004), and so according to our definition in Section 1.1 are not actually motion models. Such models still have a number of possible uses, including studying respiratory motion and how it varies between individuals with and without different pathologies. Also, these models could potentially be used for indirect correspondence models.

When using cross-population models the motion estimates should be transformed from the model space into the subject space. This can be done by registering the model's reference volume to the subject's reference volume, e.g. Ehrhardt et al. (2011).

---

[3] http://www.accuray.com/products/cyberknife-vsi-system.

This means it is necessary to acquire a reference volume for each subject. The cross-population motion estimates can be individualised for new subjects in different ways. Some papers propose modelling an average respiratory cycle and then scaling the deformations to account for how deeply the subject is breathing (Ehrhardt et al., 2008, 2011). Some papers use a statistical model (based on PCA) and then optimise the model parameters to best fit a new subject (Ehrhardt et al., 2010). The cross-population models that use direct correspondence models will individualise the motion estimates using the surrogate signals (Fayad et al., 2009a, 2010; He et al., 2010; Klinder et al., 2009, 2012; Preiswerk et al., 2012).

6. Discussion

6.1. Summary

In this paper we have presented a review of the state of the art in the field of respiratory motion modelling. In the past 15 years a range of different modelling techniques have been proposed for dealing with the effects of breathing motion in various applications, and much progress has been made. We have attempted to summarise this progress, relate techniques proposed for different application areas and highlight some of the key papers and key concepts involved in developing respiratory motion models. The aim has been to provide a timely review to inform current research and also to provide some pointers for possible future research directions.

One reason for the wide range of different techniques proposed is that requirements and restrictions vary between different applications. For example, in motion corrected MR imaging there is significant flexibility in the choice of respiratory surrogates due to the use of MR navigator echoes, but in image-guided cardiac interventions it can be challenging to acquire even a single surrogate signal. Therefore, it is not easy to provide a definitive answer to the question of 'what is the best type of motion model to use?' A number of factors will impact on this decision:

- What are the accuracy and robustness requirements for the model?
- What motion data are available for forming the model? For example, what type of breathing variation is sampled by the images used to form the model? How much control do we have over this?
- What surrogate data can reasonably be acquired to form and apply the model? How does this impact on the type of breathing variation that can be estimated?
- What type of breathing variation is it desirable to be able to estimate? This question is closely linked to the accuracy and robustness requirements of the motion model.

Based on answers to the above questions, appropriate surrogate data, an appropriate motion representation, and an appropriate correspondence model should be selected. The accuracy and robustness requirements will affect how complex the models need to be (e.g. what types and how much variation to include in the model). More complex models may enable more accurate estimates but may also be less robust to unexpected variation in the breathing and may require more data to reliably fit the model.

6.2. Breathing variation

If motion estimates need to be made over multiple breathing cycles then a strategy for dealing with the problem of inter-cycle variation must be adopted. The first possibility (and perhaps the most common found in the literature) is to ignore it. In many cases this may be the only option because of restrictions in the availability of imaging and surrogate data to form and apply the model. In addition, if there is good reason to believe that the estimation errors caused by the presence of inter-cycle variation will be small compared to the accuracy requirement of the model then this may well be the best solution. Further investigation is required to quantify the impact of inter-cycle variation in different organs and under different conditions.

The second possibility is to attempt to control the variation. Strategies for controlling inter-cycle variation could include coaching the subject to breathe more regularly, perhaps using some kind of audio and/or visual feedback (Hughes et al., 2008). Such methods are promising but require further investigation to establish how much the variation can be reduced. In addition, they will not be practical in all situations.

The third possibility for handling inter-cycle variation is to incorporate it into the model. Incorporating the variation into the model limits the choices that can be made for the surrogate data and correspondence model. Specifically, more than one independent surrogate value must be used to fully capture inter-cycle variation. Therefore, a correspondence model capable of making motion estimates based on these multiple surrogate signals should be used.

In addition, the nature of the inter-cycle variation may change when applying the model over long periods of time, so it may be necessary to devise strategies to detect when the model becomes less accurate and to use adaptive fitting (see Section 5.4).

Whichever strategy is adopted, it is a good idea to try to measure the expected variation, i.e. acquire images over several breathing cycles. Then the consequences of ignoring/controlling/modelling the variation can be assessed. However, it is not always feasible to measure the expected variation, particularly if using ionising imaging modalities such as X-ray or CT, or if the models are intended to be used over long time frames.

6.3. Validation

An important issue for any motion model is how to validate its robustness and accuracy. This paper has shown that motion models have been proposed that, in theory, are able to deal with varying degrees of the complex variation in respiratory motion. However, inaccuracies inevitably remain and it is an open research question as to precisely what the causes are of these inaccuracies and how they can be reduced. Errors in motion estimation can be caused by a number of factors, including lack of temporal/spatial resolution in the imaging data used to form the model, artefacts in these images, errors in acquiring the surrogate data used to apply the model (which may itself be imaging data) or errors introduced by the modelling process. Trade-offs may be possible in the temporal and spatial resolution of the imaging data, but the complexity of the interaction between these different error sources means that reducing inaccuracies remains a challenging task. In addition, validation is an important issue for techniques that can model and estimate breathing variation, whether it be intra-cycle, inter-cycle, inter-fraction or inter-patient variation. As discussed in Section 5.2, it is desirable that such models adequately sample the type of variation that they are attempting to model. However, in addition it is essential that the data used to validate the model also adequately samples the same variation. Such models and validation could be a useful source of information to reliably quantify the impact of the different types of variation, an area which has been relatively little studied to date.

A common approach for validating motion models in the literature has been to use some form of cross validation, most often a leave-one-out test. Although a commonly accepted validation

technique in many applications it is arguably not the most appropriate one for validating respiratory motion estimation. Motion states encountered during a single breathing cycle are not independent since they represent a continuous progression of breathing positions from end-exhalation to end-inhalation and back to end-exhalation again. Therefore, when leaving out a single motion state this lack of independence may bias the validation. It may be that approaches such as leaving out one breathing cycle (Gao et al., 2008), or separating the total data into larger sequences of training and test data may be more appropriate. Examples of such an approach include Zhang et al. (2007), in which data from a different fraction of RT was used to validate a model formed from data acquired during treatment planning; and King et al. (2008a) in which a model was formed from a single breathing type (e.g. normal, fast, deep) and validated using data acquired during other breathing types.

6.4. Indirect correspondence models

Indirect correspondence models (i.e. image driven approaches) have become more popular in recent years. This has been driven partly by the greater anticipated availability of real-time imaging data during image guided interventions. In addition to imaging data, technology now exists to acquire large amounts of surface points in real-time,[4] which could also be used to apply indirect correspondence models. Such real-time imaging/surface data is an attractive potential source of information about breathing variation (intra-cycle and inter-cycle) and some promising initial work has been performed (Vandemeulebroucke et al., 2009; Schneider et al., 2010; Li et al., 2011a; King et al., 2012; Peressutti et al., 2012). However, much work remains to be done to investigate how such imaging data can be combined with appropriate correspondence models to make fast, accurate and robust estimates of breathing motion.

6.5. Translation to the clinic

At the time of writing, almost all respiratory motion model techniques that have been described in the literature remain as research proposals. There has been very little uptake of these techniques into clinically used systems. To the authors' knowledge the only technique currently in widespread clinical use is that used by the Cyberknife[5] system for radiotherapy. There are several possible reasons for this lack of translation from research to the clinic. First, the techniques may not yet be trusted by clinicians, due to a lack of accuracy or robustness. Thorough validation of proposed approaches using clinically realistic data is therefore of paramount importance, and there is a clear need for more comparative studies of different modelling approaches. Second, they may impact too much on the clinical workflow. For example, there is often a requirement to acquire extra images to form the model and extra surrogate data to apply it. Third, and related to the second point, in many applications clinicians have adapted their practice to cope with the problems caused by respiratory motion, and so can be reluctant to adopt unproven solutions. All of these obstacles should be seen as challenges to be addressed by researchers working in the field.

6.6. Latency

One issue that must be addressed in many applications in order to develop a practical system is that of latency. Latency refers to any delay in acquiring the surrogate data, processing it to produce a motion estimate and using the estimate to guide an intervention

or perform prospective motion correction in image acquisition. Such delays can have a significant detrimental effect on the accuracy of the system. Therefore, 'predict-ahead' techniques that can estimate future motion states based on current and previous states are of interest, but were deemed beyond the scope of this review paper. One area that may be promising for future investigation could be how to combine correspondence models with such predict-ahead models, e.g. Arnold et al. (2011) and Isaksson et al. (2005). A single model could then be used estimate the motion a short time in the future from the current surrogate data.

6.7. Emerging applications and future research

Future work on respiratory motion modelling is also likely to be driven by the emergence of new potential application areas. For example, the recent development of a whole-body simultaneous PET-MR imaging system (the Biograph mMR from Siemens) has led to the possibility of using MR-derived motion models to motion correct PET data (King et al., 2011, 2012). Another potential application area where motion modelling could become key is in proton and other heavy-ion therapies (Bert and Durante, 2011). Unlike standard (photon based) RT, the requirement for accuracy is much higher in proton therapy, and the usual approach of just using larger margins around the target is not suitable.

Regarding areas for future methodological research, the concepts of indirect correspondence models and the combination of correspondence models with predict-ahead models have already been highlighted above. In addition to these a fruitful area for future research may lie in devising ways to improve the translation of motion models into clinical practice, in particular:

- A greater focus on ways of integrating motion models into clinical workflows. This will involve devising ways of forming or personalising models either using existing data or minimal amounts of additional data.
- More focus on clinically relevant validation: both retrospectively to evaluate whether models can perform well on clinically realistic data, and prospectively to detect when performance becomes unacceptable during model application.

References

Ablitt, N.A., Gao, J., Keegan, J., Stegger, L., Firmin, D.N., Yang, G.Z., 2004. Predictive cardiac motion modelling and correction with partial least squares regression. IEEE Transactions on Medical Imaging 23, 1315–1324.

Ahn, S., Yi, B., Suh, Y., Kim, J., Lee, S., Shin, S., Shin, S., Choi, E., 2004. A feasibility study on the prediction of tumour location in the lung from skin motion. British Journal of Radiology 77, 588–596.

---

[4] http://www.visionrt.com
[5] http://www.accuray.com/products/cyberknife-vsi-system.

Ambwani, S., Karl, W.C., Tawakol, A., Pien, H., 2011. Joint cardiac and respiratory motion correction and super-resolution reconstruction in coronary PET/CT. In: Proceedings International Symposium on Biomedical Imaging (ISBI), pp. 1702–1705.

Arnold, P., Preiswerk, F., Fasel, B., Salomir, R., Scheffler, K., Cattin, P.C., 2011. 3D organ motion prediction for MR guided high intensity focused ultrasound. In: Proceedings Medical Image Computing and Computer-Assisted Interventions (MICCAI).

Atkinson, D., Burcher, M., DeClerck, J., Noble, J.A., 2001. Respiratory motion compensation for 3-D freehand echocardiography. Ultrasound in Medicine and Biology 27, 1615–1620.

Batchelor, P.G., Atkinson, D., Irarrazaval, P., Hill, D.L.G., Hajnal, J., Larkman, D., 2005. Matrix description of general motion correction applied to multishot images. Magnetic Resonance in Medicine 54, 1273–1280.

Beddar, A.S., Kainz, K., Briere, T.M., Tsunashima, Y., Pan, T., Prado, K., Mohan, R., Gillin, M., Krishnan, S., 2007. Correlation between internal fiducial tumor motion and external marker motion for liver tumors imaged with 4D-CT. International Journal of Radiation Oncology Biology Physics 67, 630–638.

Benchetrit, G., 2000. Breathing pattern in humans: diversity and individuality. Respiration Physiology 122, 123–129.

Berbeco, R.I., Nishioka, S., Shirato, H., Chen, G.T.Y., Jiang, S.B., 2005. Residual motion of lung tumours in gated radiotherapy with external respiratory surrogates. Physics in Medicine and Biology 50, 3655–3667.

Bert, C., Durante, M., 2011. Motion in radiotherapy: particle therapy. Physics in Medicine and Biology 56, R113–R144.

Blackall, J.M., Ahmad, S., Miquel, M.E., McClelland, J.R., Landau, D.B., Hawkes, D.J., 2006. MRI-based measurements of respiratory motion variability and assessment of imaging strategies for radiotherapy planning. Physics in Medicine and Biology 51, 4147–4169.

Blackall, J.M., King, A.P., Penney, G.P., Adam, A., Hawkes, D.J., 2001. A statistical model of respiratory motion and deformation of the liver. In: Proceedings Medical Image Computing and Computer-Assisted Interventions (MICCAI), pp. 1338–1340.

Blackall, J.M., Penney, G.P., King, A.P., Hawkes, D.J., 2005. Alignment of sparse freehand 3-D ultrasound with preoperative images of the liver using models of respiratory motion. IEEE Transactions on Medical Imaging 24, 1405–1416.

Blume, M., Martinez-Möller, A., Keil, A., Navab, N., Rafecas, M., 2010. Joint reconstruction of image and motion in gated positron emission tomography. IEEE Transactions on Medical Imaging 29, 1892–1906.

Brock, K.K., 2010. Results of a multi-institution deformable registration accuracy study (MIDRAS). International Journal of Radiation Oncology Biology Physics 76, 583–596.

Buerger, C., Clough, R., King, A.P., Schaeffter, T., Prieto, C., 2012. Non-rigid motion modeling of the liver from 3D undersampled self-gated golden-radial phase encoded MRI. IEEE Transactions on Medical Imaging 31, 805–815.

Buerger, C., Schaeffter, T., King, A.P., 2011. Hierarchical adaptive local affine registration for fast and robust respiratory motion estimation. Medical Image Analysis 15, 551–564.

Buliev, I.G., Badea, C.T., Kolitsi, Z., Pallikarakis, N., 2003. Estimation of the heart respiratory motion with applications for cone beam computed tomography imaging: a simulation study. IEEE Transactions on Information Technology in Biomedicine 7, 404–411.

Castillo, E., Castillo, R., Martinez, J., Shenoy, M., Guerrero, T., 2010. Four-dimensional deformable image registration using trajectory modelling. Physics in Medicine and Biology 55, 305–327.

Cervino, L.I., Chao, A.K.Y., Sandhu, A., Jiang, S.B., 2009. The diaphragm as an anatomic surrogate for lung tumor motion. Physics in Medicine and Biology 54, 3529–3541.

Cervino, L.I., Jiang, Y., Sandhu, A., Jiang, S.B., 2010. Tumor motion prediction with the diaphragm as a surrogate: a feasibility study. Physics in Medicine and Biology 55, N221–N229.

Chi, P.C.M., Balter, P., Luo, D., Mohan, R., Pan, T., 2006. Relation of external surface to internal tumor motion studied with cine CT. Medical Physics 33, 3116–3123.

Cho, B., Poulsen, P.R., Keall, P.J., 2010. Real-time tumor tracking using sequential kV imaging combined with respiratory monitoring: a general framework applicable to commonly used IGRT systems. Physics in Medicine and Biology 55, 3299–3316.

Cho, B., Poulsen, P.R., Sawant, A., Ruan, D., Keall, P.J., 2011. Real-time target position estimation using stereoscopic kilovoltage/megavoltage imaging and external respiratory monitoring for dynamic multileaf collimator tracking. International Journal of Radiation Oncology Biology Physics 79, 269–278.

Cho, B., Suh, Y., Dieterich, S., Keall, P.J., 2008. A monoscopic method for real-time tumour tracking using combined occasional X-ray imaging and continuous respiratory monitoring. Physics in Medicine and Biology 53, 2837–2855.

Christensen, G.E., Rabbitt, R.D., Miller, M.I., 1996. Deformable templates using large deformation kinematics. IEEE Transactions on Image Processing 5, 1435–1447.

Chung, A.J., Camici, P.G., Yang, G.Z., 2008. Cardiac PET motion correction using materially constrained transform models. In: Proceedings Medical Imaging and Augmented Reality (MIAR), pp. 193–201.

Cline, H.E., Schenck, J.F., Hynynen, K., Watkins, R.D., Souza, S.P., Jolesz, F.A., 1992. MR-guided focused ultrasound surgery. Journal of Computer Assisted Tomography 16, 956–965.

Colgan, R., McClelland, J., McQuaid, D., Evans, P.M., Hawkes, D., Brock, J., Landau, D., Webb, S., 2008. Planning lung radiotherapy using 4D CT data and a motion model. Physics in Medicine and Biology 52, 5815–5830.

Danias, P.G., McConnell, M.V., Khasgiwala, V.C., Chuang, M.L., Edelman, R.R., Manning, W.J., 1989. Prospective navigator correction of image position for coronary MR angiography. Radiology 173, 255–263.

De Troyer, A., Estenne, M., 1984. Coordination between rib cage muscles and diaphragm during quiet breathing in humans. Journal of Applied Physiology 57, 899–906.

Ehrhardt, J., Werner, R., Frenzel, T., Sring, D., Lu, W., Low, D., Handels, H., 2007. Optical flow based method for improved reconstruction of 4d ct data sets acquired during free breathing. Medical Physics 34, 711–721.

Ehrhardt, J., Werner, R., Schmidt-Richberg, A., Handels, H., 2010. Statistical shape and motion model for the prediction of respiratory lung motion. In: Proceedings SPIE Medical Imaging.

Ehrhardt, J., Werner, R., Schmidt-Richberg, A., Handels, H., 2011. Statistical modeling of 4D respiratory lung motion using diffeomorphic image registration. IEEE Transactions on Medical Imaging 30, 251–265.

Ehrhardt, J., Werner, R., Schmidt-Richberg, A., Schulz, B., Handels, H., 2008. Generation of a mean motion model of the lung using 4DCT image data. In: Eurographics Workshop on Visual Computing for Biomedicine, pp. 69–76.

Ernst, F., Bruder, R., Schlaefer, A., Schweikard, A., 2011. Correlation between external and internal respiratory motion: a validation study. International Journal of Computer Assisted Radiology and Surgery.

Ernst, F., Martens, V., Schlichting, S., Beširević, A., Kleemann, M., Koch, C., Petersen, D., Schweikard, A., 2009. Correlating chest surface motion to motion of the liver using ε-SVR – a porcine study. In: Proceedings Medical Image Computing and Computer-Assisted Interventions (MICCAI), pp. 356–364.

Ernst, F., Schweikard, A., 2009. A survey of algorithms for respiratory motion prediction in robotic radiosurgery. In: Lecture Notes in Informatics, pp. 1035–1043.

Fayad, H., Clement, J.F., Pan, T., Roux, C., Rest, C.C.L., Pradier, O., Visvikis, D., 2009a. Towards a generic respiratory motion model for 4D CT imaging of the thorax, in: Proceedings IEEE Nuclear Science Symposium/Medical Imaging Conference.

Fayad, H., Pan, T., Clement, J.F., Visvikis, D., 2011. Technical note: correlation of respiratory motion between external patient surface and internal anatomical landmarks. Medical Physics 38, 3157–3164.

Fayad, H., Pan, T., Roux, C., Rest, C.C.L., Pradier, O., Clement, J.F., Visvikis, D., 2009b. A patient specific respiratory model based on 4D CT data and a time of flight camera (TOF). In: Proceedings IEEE Nuclear Science Symposium/Medical Imaging Conference.

Fayad, H., Pan, T., Roux, C., Rest, C.C.L., Pradier, O., Visvikis, D., 2009c. A 2D-spline patient specific model for use in radiation therapy. In: Proceedings International Symposium on Biomedical Imaging (ISBI), pp. 590–593.

Fayad, H., Pan, T., Roux, C., Visvikis, D., 2010. A generic respiratory motion model for motion correction in PET/CT. In: Proceedings IEEE Nuclear Science Symposium/ Medical Imaging Conference, pp. 2455–2458.

Filipovic, M., Vuissoz, P.A., Codreanu, A., Claudon, M., Felblinger, J., 2011. Motion compensated generalized reconstruction for free-breathing dynamic contrast-enhanced MRI. Magnetic Resonance in Medicine 65, 812–822.

Fischer, R.W., Botnar, R.M., Nehrke, K., Boesiger, P., Manning, W.J., Peters, D.C., 2006. Analysis of residual coronary artery motion for breath hold and navigator approaches using real-time coronary MRI. Magnetic Resonance in Medicine 55, 612–618.

Gao, G., McClelland, J., Tarte, S., Blackall, J., Hawkes, D., 2008. Modelling the respiratory motion of the internal organs by using canonical correlation analysis and dynamic MRI. In: The First International Workshop on Pulmonary Image Analysis held at MICCAI 2008.

Geneser, S., Hinkle, J., Kirby, R., Wang, B., Salter, B., Joshi, S., 2011. Quantifying variability in radiation dose due to respiratory-induced tumor motion. Medical Image Analysis 15, 640–649.

Grossman, W., 1986. Cardiac Catheterization and Angiography. Lea and Febiger.

Hawkes, D.J., Barratt, D., Blackall, J.M., Chan, C., Edwards, P.J., Rhode, K., Penney, G.P., McClelland, J., Hill, D.L.G., 2005. Tissue deformation and shape models in image-guided interventions: a discussion paper. Medical Image Analysis 9, 163–175.

He, T., Xue, Z., Xie, W., Wong, S.T., 2010. Online 4-D CT estimation for patient-specific respiratory motion based on real-time breathing signals. In: Proceedings Medical Image Computing and Computer-Assisted Interventions (MICCAI).

Henningsson, M., Koken, P., Stehning, C., Razavi, R., Prieto, C., Botnar, R.M., 2012. Whole-heart coronary MR angiography with 2D self-navigated image reconstruction. Magnetic Resonance in Medicine 67, 437–445.

Hinkle, J., Fletcher, P.T., Wang, B., Salter, B., Joshi, S., 2009. 4D MAP image reconstruction incorporating organ motion. In: Proceedings Information Processing in Medical Imaging (IPMI), pp. 676–687.

Hoisak, J.D.P., Sixel, K.E., Tirona, R., Cheung, P.C.F., philippe Pignol, J., 2004. Correlation of lung tumour motion with external surrogate indicators of respiration. International Journal of Radiation Oncology Biology Physics 60, 1298–1306.

Hoogeman, M., briac Prévost, J., Nuyttens, J., Levendag, J.P.P., Heijmen, B., 2009. Clinical accuracy of the respiratory tumor tracking system of the cyberknife: assessment by analysis of log files. International Journal of Radiation Oncology Biology Physics 74, 297–303.

Horn, B.K., Schunck, B.G., 1981. Determining optical flow. Artificial Intelligence 17, 185–203.

Huang, J., Abendschein, D., ávila Román, V.G.D., Amini, A.A., 1999. Spatio-temporal tracking of myocardial deformations with a 4-D B-spline model from tagged MRI. IEEE Transactions on Medical Imaging 18, 957–972.

Hughes, S., McClelland, J., Tarte, S., Blackall, J., Liong, J., Ahmad, S., Hawkes, D., Landau, D., 2008. Assessment of respiratory cycle variability with and without training using a visual guide. Cancer Therapy 6, 945–954.

Hughes, S., McClelland, J., Tarte, S., Lawrence, D., Ahmad, S., Hawkes, D., Landau, D., 2009. Assessment of two novel ventilatory surrogates for use in the delivery of gated/tracked radiotherapy for non-small cell lung cancer. Radiotherapy and Oncology 91, 336–341.

Ionascu, D., Jiang, S.B., Nishioka, S., Shirato, H., Berbeco, R.I., 2007. Internal–external correlation investigations of respiratory induced motion of lung tumors. Medical Physics 34, 3893–3903.

Isaksson, M., Jalden, J., Murphy, M.J., 2005. On using an adaptive neural network to predict lung tumor motion during respiration for radiotherapy applications. Medical Physics 32, 3801–3809.

Jahnke, C., Nehrke, K., Paetsch, I., Schnackenburg, B., Gebker, R., Fleck, E., Nagel, E., 2007. Improved bulk myocardial motion suppression for navigator-gated coronary magnetic resonance imaging. Journal of Magnetic Resonance Imaging 26, 780–786.

Jahnke, C., Paetsch, I., Nehrke, K., Schnackenburg, B., Gebker, R., Fleck, E., 2005. Rapid and complete coronary arterial tree visualization with magnetic resonance imaging: feasibility and diagnostic performance. European Heart Journal 26, 2313–2319.

Jolliffe, I.T., 2002. Principal Component Analysis (Springer Series in Statistics). Springer.

Kalman, R.E., 1960. A new approach to linear filtering and prediction problems. Transactions of the ASME Journal of Basic Engineering 82, 35–45.

Keall, P.J., Mageras, G.S., Balter, J.M., Emery, R.S., Forster, K.M., Jiang, S.B., Kapatoes, J.M., Low, D.A., Murphy, M.J., Murray, B.R., Ramsey, C.R., Herk, M.B.V., Vedam, S.S., Wong, J.W., Yorke, E., 2006. The management of respiratory motion in radiation oncology report of AAPM task group 76. Medical Physics 33, 3874–3900.

Keall, P.J., Starkschall, G., Shukla, H., Forster, K.M., Ortiz, V., Stevens, C.W., Vedam, S.S., George, R., Guerrero, T., Mohan, R., 2004. Acquiring 4D thoracic CT scans using a multislice helical method. Physics in Medicine and Biology 49, 2053–2067.

Keegan, J., Gatehouse, P.D., Yang, G.Z., Firmin, D.N., 2007. Non-model-based correction of respiratory motion using beat-to-beat 3D spiral fat-selective imaging. Journal of Magnetic Resonance Imaging 26, 624–629.

Khamene, A., Warzelhan, J.K., Vogt, S., Elgort, D., ChefdHotel, C., Duerk, J.L., Lewin, J., Wacker, F.K., Sauer, F., 2004. Characterization of internal organ motion using skin marker positions. In: Proceedings Medical Image Computing and Computer-Assisted Interventions (MICCAI), pp. 526–533.

King, A.P., Blackall, J.M., Penney, G.P., Hawkes, D.J., 2001. Tracking liver motion using 3-D ultrasound and a surface based statistical shape model. In: Proceedings Mathematical Methods in Biomedical Image Analysis (MMBIA), pp. 145–152.

King, A.P., Boubertakh, R., Ng, K.L., Ma, Y.L., Chinchapatnam, P., Gao, G., Schaeffter, T., Hawkes, D.J., Razavi, R., Rhode, K.S., 2008a. A technique for respiratory motion correction in image guided cardiac catheterisation procedures. In: Proceedings SPIE Medical Imaging.

King, A.P., Boubertakh, R., Rhode, K.S., Ma, Y.L., Chinchapatnam, P., Gao, G., Tangcharoen, T., Ginks, M., Cooklin, M., Gill, J.S., Hawkes, D.J., Razavi, R.S., Schaeffter, T., 2009a. A subject-specific technique for respiratory motion correction in image-guided cardiac catheterisation procedures. Medical Image Analysis 13, 419–431.

King, A.P., Buerger, C., Schaeffter, T., 2010a. Cardiac respiratory motion modelling by simultaneous registration and modelling from dynamic MRI images. In: Proceedings Workshop on Biomedical Image Registration (WBIR), pp. 222–233.

King, A.P., Buerger, C., Tsoumpas, C., Marsden, P., Schaeffter, T., 2012. Thoracic respiratory motion estimation from MRI using a statistical model and a 2-D image navigator. Medical Image Analysis 16, 252–264.

King, A.P., Jansen, C., Boubertakh, R., Rhode, K.S., Razavi, R., Penney, G.P., 2008b. Model-based respiratory motion correction using 3-D echocardiography. In: Proceedings International Symposium on Biomedical Imaging (ISBI), pp. 1465–1468.

King, A.P., Jansen, C., Rhode, K.S., Caulfield, D., Razavi, R.S., Penney, G.P., 2010b. Respiratory motion correction for image-guided cardiac interventions using 3-D echocardiography. Medical Image Analysis 14, 21–29.

King, A.P., Rhode, K.S., Ma, Y., Yao, C., Jansen, C., Razavi, R., Penney, G.P., 2010c. Registering preprocedure volumetric images with intraprocedure 3-D ultrasound using an ultrasound imaging model. IEEE Transactions on Medical Imaging 29, 924–937.

King, A.P., Rhode, K.S., Razavi, R.S., Schaeffter, T.R., 2009b. An adaptive and predictive respiratory motion model for image-guided interventions: theory and first clinical application. IEEE Transactions on Medical Imaging 28, 2020–2032.

King, A.P., Tsoumpas, C., Buerger, C., Schulz, V., Marsden, P., Schaeffter, T., 2011. Real-time respiratory motion correction for simultaneous PET-MR using an MR-derived motion model. In: Proceedings IEEE Nuclear Science Symposium/Medical Imaging Conference.

Klein, G.J., Reutter, B.W., Huesman, R.H., 2001. Four-dimensional affine registration models for respiratory-gated PET. IEEE Transactions on Nuclear Science 48, 756–760.

Klinder, T., Lorenz, C., 2012. Respiratory motion compensation for image-guided bronchoscopy using a general motion model. In: Proceedings International Symposium on Biomedical Imaging (ISBI).

Klinder, T., Lorenz, C., Ostermann, J., 2009. Free-breathing intra- and intersubject respiratory motion capturing, modeling, and prediction. In: Proceedings SPIE Medical Imaging.

Klinder, T., Lorenz, C., Ostermann, J., 2010. Prediction framework for statistical respiratory motion modelling. In: Proceedings Medical Image Computing and Computer-Assisted Interventions (MICCAI), pp. 327–334.

Koch, N., Liu, H.H., Starkschall, G., Jacobson, M., Forster, K., Liao, Z., Komaki, R., Stevens, C.W., 2004. Evaluation of internal lung motion for respiratory-gated radiotherapy using MRI: Part i. Correlating internal lung motion with skin fiducial motion. International Journal of Radiation Oncology Biology Physics 60, 1459–1472.

Konno, K., Mead, J., 1967. Measurement of the separate volume changes of rib cage and abdomen during breathing. Journal of Applied Physiology 22, 407–422.

Li, G., Arora, N.C., Xie, H., Ning, H., Lu, W., Low, D., Citrin, D., Kaushal, A., Zach, L., Camphausen, K., Miller, R.W., 2009. Quantitative prediction of respiratory tidal volume based on the external torso volume change: a potential volumetric surrogate. Physics in Medicine and Biology 54, 253–267.

Li, R., Lewis, J.H., Jia, X., Gu, X., Folkerts, M., Men, C., Song, W.Y., Jiang, S.B., 2011a. 3D tumor localization through real-time volumetric X-ray imaging for lung cancer radiotherapy. Medical Physics 38, 2783–2794.

Li, R., Lewis, J.H., Jia, X., Zhao, T., Liu, W., Wuenschel, S., Lamb, J., Yang, D., Low, D.A., Jiang, S.B., 2011b. On a PCA-based lung motion model. Physics in Medicine and Biology 56, 6009–6030.

Li, T., Schreibmann, E., Yang, Y., L, X., 2006a. Motion correction for improved target localization with on-board cone-beam computed tomography. Physics in Medicine and Biology 51, 253–267.

Li, T., Thorndyke, B., Schreibmann, E., Yang, Y., Xing, L., 2006b. Model-based image reconstruction for four-dimensional PET. Medical Physics 33, 1288–1298.

Liu, H.H., Koch, N., Starkschall, G., Jacobson, M., Forster, K., Liao, Z., Komaki, R., Stevens, C.W., 2004. Evaluation of internal lung motion for respiratory-gated radiotherapy using MRI: Part II. Margin reduction of internal target volume. International Journal of Radiation Oncology Biology Physics 60, 1473–1483.

Liu, X., Oguz, I., Pizer, S.M., Mageras, G.S., 2010. Shape-correlated deformation statistics for respiratory motion prediction in 4D lung. In: Proceedings SPIE Medical Imaging.

Low, D.A., Parikh, P., Lu, W., Dempsey, J., Wahab, S., Hubenschmidt, J., Nystrom, M., Handoko, M., Bradley, J., 2005. Novel breathing motion model for radiotherapy. International Journal of Radiation Oncology Biology Physics 63, 921–929.

Low, D.A., Zhao, T., White, B., Yang, D., Mutic, S., Noel, C.E., Bradley, J.D., Parikh, P.J., Lu, W., 2010. Application of the continuity equation to a breathing motion model. Medical Physics 37, 1360–1364.

Lu, W., Low, D.A., Parikh, P.J., Nystrom, M.M., El Naqa, I.M., Wahab, S.H., Handoko, M., Fooshee, D., Bradley, J.D., 2005. Comparison of spirometry and abdominal height as four-dimensional computed tomography metrics in lung. Medical Physics 32, 2351–2357.

Lynn, J.G., Zwemer, R.L., Chick, A.J., Miller, A.E., 1942. A new method for the generation and use of focused ultrasound in experimental biology. Journal of General Physiology 26, 179–193.

Makela, T., Clarysse, P., Sipila, O., Pauna, N., Pham, Q.C., Katila, T., Magnin, I., 2002. A review of cardiac image registration methods. IEEE Transactions on Medical Imaging 21, 1011–1021.

Manke, D., Nehrke, K., Bornert, P., 2003. Novel prospective respiratory motion correction approach for free-breathing coronary MR angiography using a patient-adapted affine motion model. Magnetic Resonance in Medicine 50, 122–131.

Manke, D., Nehrke, K., Börnert, P., Rösch, P., Dössel, O., 2002a. Respiratory motion in coronary magnetic resonance angiography: a comparison of different motion models. Journal of Magnetic Resonance Imaging 15, 661–671.

Manke, D., Rosch, P., Nehrke, K., Bornert, P., Dossel, O., 2002b. Model evaluation and calibration for prospective respiratory motion correction in coronary MR angiography based on 3-D image registration. IEEE Transactions on Medical Imaging 21, 1132–1141.

Martin, J., McClelland, J., Thomas, C., Wildermuth, K., Landau, D., Ourselin, S., Hawkes, D., 2012. Motion modelling and motion compensated reconstruction of tumours in cone-beam computed tomography. In: Proceedings Mathematical Methods in Biomedical Image Analysis (MMBIA).

McClelland, J.R., Chandler, A.G., Blackall, J.M., Ahmad, S., Landau, D., Hawkes, D.J., 2005. 4D motion models over the respiratory cycle for use in lung cancer radiotherapy planning. In: Proceedings SPIE Medical Imaging.

McClelland, J.R., Chandler, A.G., Blackall, J.M., Tarte, S., Hughes, S., Ahmad, S., Landau, D., Hawkes, D.J., 2006. A continuous 4D motion model from multiple respiratory cycles for use in lung radiotherapy. Medical Physics 33, 3348–3358.

McClelland, J.R., Hughes, S., Modat, M., Qureshi, A., Ahmad, S., Landau, D.B., Ourselin, S., Hawkes, D.J., 2011. Inter-fraction variations in respiratory motion models. Physics in Medicine and Biology 56, 251–272.

McClelland, J.R., Webb, S., McQuaid, D., Binnie, D.M., Hawkes, D.J., 2007. Tracking differential organ motion with a breathing multileaf collimator: magnitude of problem assessed using 4D CT data and a motion-compensation strategy. Physics in Medicine and Biology 52, 4805–4826.

McGahan, J.P., Browning, P.D., Brock, J., Teslik, H., 1990. Hepatic ablation using radiofrequency electrocautery. Investigative Radiology 25, 267–270.

McGlashan, N., King, A.P., 2011. Capturing breathing motion variability using two signal motion models of the heart. In: Proceedings Medical Image Understanding and Analysis (MIUA).

McLeish, K., Hill, D.L.G., Atkinson, D., Blackall, J.M., Razavi, R., 2002. A study of the motion and deformation of the heart due to respiration. IEEE Transactions on Medical Imaging 21, 1142–1150.

McQuaid, S.J., Lambrou, T., Cunningham, V.J., Bettinardi, V., Gilardi, M.C., Hutton, B.F., 2009. The application of a statistical shape model to diaphragm tracking in respiratory-gated cardiac PET images. Proceedings of the IEEE 97, 2039–2052.

McQuaid, S.J., Lambrou, T., Hutton, B.F., 2011. A novel method for incorporating respiratory-matched attenuation correction in the motion correction of cardiac PET-CT studies. Physics in Medicine and Biology 56, 2903–2915.

Metz, C.T., Klein, S., Schaap, M., van Walsum, T., Niessen, W.J., 2011. Nonrigid registration of dynamic medical imaging data using nD + t B-splines and a groupwise optimization approach. Medical Image Analysis 15, 238–249.

Meyer, J., Baier, K., Wilbert, J., Guckenberger, M., Richter, A., Flentje, M., 2006. Three-dimensional spatial modelling of the correlation between abdominal motion and lung tumour motion with breathing. Acta Oncologica 45, 923–934.

Murphy, K., van Ginneken, B., Reinhardt, J., Kabus, S., Ding, K., Deng, X., Cao, K., Du, K., Christensen, G., Garcia, V., Vercauteren, T., Ayache, N., Commowick, O., Malandain, G., Glocker, B., Paragios, N., Navab, N., Gorbunova, V., Sporring, J., de Bruijne, M., Han, X., Heinrich, M., Schnabel, J., Jenkinson, M., Lorenz, C., Modat, M., McClelland, J., Ourselin, S., Muenzing, S., Viergever, M., De Nigris, D., Collins, D., Arbel, T., Peroni, M., Li, R., Sharp, G., Schmidt-Richberg, A., Ehrhardt, J., Werner, R., Smeets, D., Loeckx, D., Song, G., Tustison, N., Avants, B., Gee, J., Staring, M., Klein, S., Stoel, B., Urschler, M., Werlberger, M., Vandemeulebroucke, J., Rit, S., Sarrut, D., Pluim, J., 2011. Evaluation of registration methods on thoracic CT: the EMPIRE10 challenge. IEEE Transactions on Medical Imaging 30, 1901–1920.

Nehmeh, S.A., Erdi, Y.E., 2008. Respiratory motion in positron emission tomography/computed tomography: a review. Seminars in Nuclear Medicine 38, 167–176.

Nehrke, K., Bornert, P., 2005. Prospective correction of affine motion for arbitrary MR sequences on a clinical scanner. Magnetic Resonance in Medicine 54, 1130–1138.

Nehrke, K., Bornert, P., Manke, D., Bock, J.C., 2001. Free-breathing cardiac MR imaging: study of implications of respiratory motion – initial results. Radiology 220, 810–815.

Odille, F., Cîndea, N., Mandry, D., Pasquier, C., Vuissoz, P.A., Felblinger, J., 2008a. Generalized MRI reconstruction including elastic physiological motion and coil sensitivity encoding. Magnetic Resonance in Medicine 56, 1401–1411.

Odille, F., Uribe, S., Batchelor, P.G., Prieto, C., Schaeffter, T., Atkinson, D., 2010. Model-based reconstruction for cardiac cine MRI without ECG or breath holding. Magnetic Resonance in Medicine 63, 1247–1257.

Odille, F., Vuissoz, P.A., Marie, P.Y., Felblinger, J., 2008b. Generalized reconstruction by inversion of coupled systems (GRICS) applied to free-breathing MRI. Magnetic Resonance in Medicine 60, 146–157.

Pan, T., Lee, T.Y., Rietzel, E., Chen, G.T.Y., 2004. 4D-CT imaging of a volume influenced by respiratory motion on multi-slice CT. Medical Physics 31, 333–340.

Peressutti, D., Rijkhorst, E.J., Barratt, D.C., Penney, G.P., King, A.P., 2012. Estimating and resolving uncertainty in cardiac respiratory motion modelling. In: Proceedings International Symposium on Biomedical Imaging (ISBI), pp. 262–265.

Plathow, C., Zimmermann, H., Fink, C., Umathum, R., Schbinger, M., Huber, P., Zuna, I., Debus, J., Schlegel, W., Peter Meinzer, H., Semmler, W., Ulrich Kauczor, H., Bock, M., 2005. Influence of different breathing maneuvers on internal and external organ motion: use of fiducial markers in dynamic MRI. International Journal of Radiation Oncology Biology Physics 62, 238–245.

Preiswerk, F., Arnold, P., Fasel, B., Cattin, P.C., 2012. Robust tumour tracking from 2D imaging using a population-based statistical motion model. In: Proceedings MMBIA.

Rahni, A.A.A., Lewis, E., Guy, M.J., Goswami, B., Wells, K., 2011. A particle filter approach to respiratory motion estimation in nuclear medicine imaging. IEEE Transactions on Nuclear Science 58, 2276–2285.

Reyes, M., Malandain, G., Koulibaly, P.M., González-Ballester, M.A., Darcourt, J., 2007. Model-based respiratory motion compensation for emission tomography image reconstruction. Physics in Medicine and Biology 52, 3579–3600.

Rijkhorst, E.J., Heanes, D., Odille, F., Hawkes, D., Barratt, D., 2010. Simulating dynamic ultrasound using MR-derived motion models to assess respiratory synchronisation for image-guided liver interventions. In: Proceedings International Conference on Information Processing in Computer-Assisted Interventions (IPCAI).

Rijkhorst, E.J., Rivens, I., ter Haar, G., Hawkes, D., Barratt, D., 2011. Effects of respiratory liver motion on heating for gated and model-based motion-compensated high-intensity focused ultrasound ablation. In: Proceedings Medical Image Computing and Computer-Assisted Interventions (MICCAI).

Rit, S., Wolthaus, J.W.H., van Herk, M., Sonke, J.J., 2009. On-the-fly motion-compensated cone-beam CT using an a priori model of the respiratory motion. Medical Physics 36, 2283–2296.

Rohlfing, T., Maurer, J.C.R., O'Dell, W.G., Zhong, J., 2004. Modeling liver motion and deformation during the respiratory cycle using intensity-based nonrigid registration of gated MR images. Medical Physics 31, 427–432.

Ruan, D., Fessler, J.A., Balter, J.M., Berbeco, R.I., Nishioka, S., Shirato, H., 2008. Inference of hysteretic respiratory tumour motion from external surrogates: a state augmentation approach. Physics in Medicine and Biology 53, 2923–2936.

Ruan, D., Fessler, J.A., Balter, J.M., Keall, P.J., 2009. Real-time profiling of respiratory motion: baseline drift, frequency variation and fundamental pattern change. Physics in Medicine and Biology 54, 4777–4792.

Rueckert, D., Sonoda, L.I., Hayes, C., Hill, D.L.G., Leach, M.O., Hawkes, D.J., 1999. Non-rigid registration using free-form deformations: application to breast MR images. IEEE Transactions on Medical Imaging 18, 712–721.

Santelli, C., Nezafat, R., Goddu, B., Manning, W.J., Smink, J., Kozerke, S., Peters, D.C., 2011. Respiratory bellows revisited for motion compensation: preliminary experience for cardiovascular MR. Magnetic Resonance in Medicine 65, 1098–1103.

Savill, F., Schaeffter, T., King, A.P., 2011. Assessment of input signal positioning for cardiac respiratory motion models during different breathing patterns. In: Proceedings International Symposium on Biomedical Imaging (ISBI), pp. 1698–1701.

Schneider, M., Sundar, H., Liao, R., Hornegger, J., Xu, C.Y., 2010. Model-based respiratory motion compensation for image-guided cardiac interventions. In: Proceedings Computer Vision and Pattern Recognition (CVPR), pp. 2948–2954.

Schreibmann, E., Thorndyke, B., Li, T., Wang, J., Xing, L., 2008. Four-dimensional image registration for image-guided radiotherapy. International Journal of Radiation Oncology Biology Physics 71, 578–586.

Schweikard, A., Glosser, G., Bodduluri, M., Murphy, M.J., Adler, J.R., 2000. Robotic motion compensation for respiratory movement during radiosurgery. Computer Aided Surgery 5, 263–277.

Schweikard, A., Shiomi, H., Adler, J., 2004a. Respiration tracking in radiosurgery. Medical Physics 31, 2738–2741.

Schweikard, A., Shiomi, H., Adler, J., 2005. Respiration tracking in radiosurgery without fiducials. International Journal of Medical Robotics and Computer Assisted Surgery 1, 19–27.

Schweikard, A., Shiomi, H., Fisseler, J., Dötter, M., Berlinger, K., Gehl, H.B., Adler, J., 2004b. Fiducial-less respiration tracking in radiosurgery. In: Proceedings Medical Image Computing and Computer-Assisted Interventions (MICCAI), pp. 992–999.

Scott, A.D., Keegan, J., Firmin, D.N., 2009. Motion in cardiovascular MR imaging. Radiology 250, 331–351.

Segars, W.P., Lalush, D.S., Tsui, B.M.W., 2001. Modeling respiratory mechanics in the MCAT and spline based MCAT phantoms. IEEE Transactions on Nuclear Science 48, 89–97.

Seppenwoolde, Y., Berbeco, R.I., Nishioka, S., Shirato, H., Heijmen, B., 2007. Accuracy of tumour motion compensation algorithm from a robotic respiratory tracking system: a simulation study. Medical Physics 34, 2774–2784.

Sharif, B., Bresler, Y., 2007. Affine-corrected paradise: free-breathing patient adaptive cardiac MRI with sensitivity encoding. In: Proceedings International Symposium on Biomedical Imaging (ISBI), pp. 1076–1079.

Sharp, J.T., Goldberg, N.B., Druz, W.S., Danon, J., 1975. Relative contributions of rib cage and abdomen to breathing in normal subjects. Journal of Applied Physiology 39, 608–618.

Shechter, G., Ozturk, C., Resar, J.R., McVeigh, E.R., 2004. Respiratory motion of the heart from free breathing coronary angiograms. IEEE Transactions on Medical Imaging 23, 1046–1056.

Shechter, G., Resar, J.R., McVeigh, E.R., 2006. Displacement and velocity of the coronary arteries: cardiac and respiratory motion. IEEE Transactions on Medical Imaging 25, 369–375.

Shechter, G., Shechter, B., Resar, J.R., Beyar, R., 2005. Prospective motion correction of X-ray images for coronary interventions. IEEE Transactions on Medical Imaging 24, 441–450.

Shirato, H., Shimizu, S., Kunieda, T., Kitamura, K., van Herk, M., Kagei, K., Nishioka, T., Hashimoto, S., Fujita, K., Aoyama, H., Tsuchiya, K., Kudo, K., Miyasaka, K., 2000. Physical aspects of a real-time tumor-tracking system for gated radiotherapy. International Journal of Radiation Oncology Biology Physics 48, 1187–1195.

Sonke, J.J., Lebesque, J., Herk, M.V., 2008. Variability of four-dimensional computed tomography patient models. International Journal of Radiation Oncology Biology Physics 70, 590–598.

Stehning, C., Börnert, P., Nehrke, K., Eggers, H., Stuber, M., 2005. Free-breathing whole-heart coronary MRA with 3D radial SSFP and self-navigated image reconstruction. Magnetic Resonance in Medicine 54, 476–480.

Sundaram, T.A., Avants, B.B., Gee, J.C., 2004. A dynamic model of average lung deformation using capacity-based reparameterization and shape averaging of lung MR images. In: Proceedings Medical Image Computing and Computer-Assisted Interventions (MICCAI), pp. 1000–1007.

Thirion, J.P., 1998. Image matching as a diffusion process: an analogy with Maxwell's demons. Medical Image Analysis 2, 243–260.

Timinger, H., Krueger, S., Borgert, J., Grewer, R., 2004. Motion compensation for interventional navigation on 3D static roadmaps based on an affine model and gating. Physics in Medicine and Biology 49, 719–732.

Torshabi, A.E., Pella, A., Riboldi, M., Baroni, G., 2010. Targeting accuracy in real-time tumor tracking via external surrogates: a comparative study. Technology in Cancer Research and Treatment 9, 1–11.

Uribe, S., Muthurangu, V., Boubertakh, R., Schaeffter, T., Razavi, R., Hill, D.L., Hansen, M.S., 2007. Whole-heart cine MRI using real-time respiratory self-gating. Magnetic Resonance in Medicine 57, 606–613.

Vandemeulebroucke, J., Kybic, J., Clarysse, P., Sarrut, D., 2009. Respiratory motion estimation from cone-beam projections using a prior model. In: Proceedings Medical Image Computing and Computer-Assisted Interventions (MICCAI).

Vandemeulebroucke, J., Rit, S., Kybic, J., Clarysse, P., Sarrut, D., 2011. Spatiotemporal motion estimation for respiratory-correlated imaging of the lungs. Medical Physics 38, 166–178.

Vedam, S.S., Kini, V.R., Keall, P.J., Ramakrishnan, V., Mostafavi, H., Mohan, R., 2003. Quantifying the predictability of diaphragm motion during respiration with a noninvasive external marker. Medical Physics 30, 505–513.

Verma, P.S., Wu, H., Langer, M.P., Das, I.J., Sandison, G., 2011. Survey: real-time tumor motion prediction for image-guided radiation treatment. Computing in Science & Engineering 13, 24–35.

Wang, Y., Riederer, S.J., Ehman, R.L., 1995. Respiratory motion of the heart: kinematics and the implications for the spatial resolution in coronary imaging. Magnetic Resonance in Medicine 33, 713–719.

West, J.B., 2004. Respiratory Physiology: The Essentials, seventh ed. Williams and Wilkins, Lippincott.

White, M.J., Hawkes, D.J., Melbourne, A., Collins, D.J., Coolens, C., Hawkins, M., Leach, M.O., Atkinson, D., 2009. Motion artifact correction in free-breathing abdominal MRI using overlapping partial samples to recover image deformations. Magnetic Resonance in Medicine 62, 440–449.

Wood, M.L., Henkelman, R.M., 1985. MR image artifacts from periodic motion. Medical Physics 12, 143–151.

Wu, Q., Chung, A.J., Yang, G.Z., 2006. Optimal sensor placement for predictive cardiac motion modelling. In: Proceedings Medical Image Computing and Computer-Assisted Interventions (MICCAI), pp. 512–519.

Xu, Q., Hamilton, R., 2006. A novel respiratory detection method based on automated analysis of ultrasound diaphragm video. Medical Physics 33, 916–921.

Yang, D., Lu, W., Low, D.A., Deasy, J.O., Hope, A.J., Naqa, I.E., 2008. 4D-CT motion estimation using deformable image registration and 5D respiratory motion modeling. Medical Physics 35, 4577–4590.

Zeng, R., Fessler, J.A., Balter, J.M., 2007. Estimating 3-D respiratory motion from orbiting views by tomographic image registration. IEEE Transactions on Medical Imaging 26, 153–163.

Zhang, Q., Hu, Y.C., Liu, F., Goodman, K., Rosenzweig, K.E., Mageras, G.S., 2010. Correction of motion artifacts in cone-beam CT using a patient-specific respiratory motion model. Medical Physics 37, 2901–2909.

Zhang, Q., Pevsner, A., Hertanto, A., Hu, Y.C., Rosenzweig, K.E., Ling, C.C., Mageras, G.S., 2007. A patient-specific respiratory model of anatomical motion for radiation treatment planning. Medical Physics 34, 4772–4781.

Zhao, T., Lu, W., Yang, D., Mutic, S., Noel, C.E., Parikh, P.J., Bradley, J.D., Low, D.A., 2009. Characterization of free breathing patterns with 5D lung motion model. Medical Physics 36, 5183–5189.

Zhu, Y., Tsin, Y., Sundar, H., Sauer, F., 2010. Image-based respiratory motion compensation for fluoroscopic coronary roadmapping. In: Proceedings Medical Image Computing and Computer-Assisted Interventions (MICCAI), pp. 287–294.